

# Holographic massive plasma state in Friedman Universe: cosmological fine-tuning and coincidence problems

**She-Sheng Xue**

ICRANet Piazzale della Repubblica, 10 -65122, Pescara, Italy  
Physics Department, Sapienza University of Rome, Rome, Italy  
INFN, Sezione di Perugia, Perugia, Italy  
ICTP-AP, University of Chinese Academy of Sciences, Beijing, China

E-mail: [xue@icra.it](mailto:xue@icra.it), [she-sheng.xue@cern.ch](mailto:she-sheng.xue@cern.ch)

**Abstract.** Massive particle and antiparticle pair production and oscillation on the horizon form a holographic and massive pair plasma state in the Friedman Universe. Via this state, the Einstein cosmology term (dark energy) interacts with matter and radiation and is time-varying  $\tilde{\Lambda}$  in the Universe's evolution. It is determined by a close set of ordinary differential equations for dark energy, matter, and radiation energy densities. The solutions are unique, provided the initial conditions given by observations. In inflation and reheating, dark energy density decreases from the inflation scale, converting to matter and radiation energy densities. In standard cosmology, matter and radiation energy densities convert to dark energy density, reaching the present Universe. By comparing with  $\Lambda$ CDM, quintessence and dark energy interacting models, we show that these results can be the possible solutions for cosmological fine-tuning and coincidence problems.

---

## Contents

<b>1</b>	<b>Introduction</b>	<b>1</b>
<b>2</b>	<b>Cosmological <math>\tilde{\Lambda}</math>CDM model</b>	<b>3</b>
2.1	Time-varying cosmological $\tilde{\Lambda}$ term	3
2.2	Massive pair production and oscillation	3
2.3	Holographic and massive pair plasma state	4
2.4	Cosmic rate equations for matter and radiation densities	4
2.5	Preliminary applications to inflation and reheating	5
<b>3</b>	<b><math>\tilde{\Lambda}</math>CDM equations of dark energy and matter interaction</b>	<b>6</b>
3.1	Dark energy interaction with matter and radiation	7
3.2	A close set of ordinary differential equations for cosmic abundance	7
3.3	Initial condition at present or reheating time	8
<b>4</b>	<b>Cosmological coincidence problem</b>	<b>9</b>
4.1	Unique solution to $\tilde{\Lambda}$ CDM equations and boundary conditions	10
4.2	Three evolution phases evading cosmological coincidence problem	12
<b>5</b>	<b>Comparison and contrast with <math>\Lambda</math>CDM and other models</b>	<b>13</b>
5.1	Contrast with $\Lambda$ CDM solutions	13
5.2	Distinct from other dark-energy interacting models	17
5.3	Comparison with quintessence tracker solutions	17
5.4	Approximated $\tilde{\Lambda}$ CDM solution for phenomenological studies	17
<b>6</b>	<b>Discussions on Einstein cosmological <math>\Lambda</math> term</b>	<b>18</b>
6.1	Geometric nature of $\tilde{\Lambda}$ dark energy as gravitational ground state	19
6.2	Asymptotically safe Einstein theory for early and present Universe	19
6.3	Dynamical nature of $\tilde{\Lambda}$ dark energy solving fine-tuning problem	20
<b>7</b>	<b>Appendix: quantum pair oscillation details</b>	<b>21</b>

---

## 1 Introduction

Einstein's equation describes the Universe's evolution in terms of Newton's constant  $G$ , Ricci scalar  $R$ , cosmological constant  $\Lambda$  and matter and radiation energy densities. Einstein introduced the  $\Lambda$  to counterbalance attractive gravity and achieve a static universe. It was abandoned after the confirmation of Universe expansion. It has been revived since the discovery of the Universe's acceleration, which implies that the  $\Lambda$  may have a positive value. Owing to its mysterious origin and nature, the  $\Lambda$  component is dubbed as "dark energy". As a standard model of the Big Bang cosmology, the simplest

$\Lambda$ CDM (Lambda cold dark matter) model provides a reasonably good account of the observed properties of the cosmos and accelerating Universe.

However, whatever the dark energy form and nature are, two cosmological problems arise in  $\Lambda$ CDM. The cosmic fine-tuning problem [1]: how to explain the present dark energy density  $\sim 10^{-47}\text{GeV}^4$  is about  $10^{-123}$  smaller than the energy density at the Planck scale  $M_{\text{pl}} = G^{-1/2} \approx 1.2 \times 10^{19}\text{GeV}$ . It is a unique basic scale entering Einstein's equation. The cosmic coincidence problem [2–4]: how to explain the coincidence of dark energy and matter densities at the present epoch after a long cosmic evolution. Observe that throughout the cosmic evolution after the Big Bang (reheating), dark energy density  $\rho_\Lambda = \Lambda^2/(8\pi G)$  does not change. While radiation and matter energy densities fall in powers of the scalar factor  $a$  and change many orders of magnitudes. In the recent epoch, their abundances  $\Omega_\Lambda \approx 0.7$  and  $\Omega_M \approx 0.3$  not only coincide in order of magnitude but also are just the correct values for forming structure, galaxy, and astrophysical objects. It is just the world where human beings create and live. There are three possibilities. (i) We are subject to the Anthropic Principle and happen to live with a peculiar  $\Lambda$  value and in a special epoch after the long history of Big Bang cosmology, (ii) Nature fine-tunes in many orders of magnitude the  $\Lambda$  value and the ratio of dark energy and radiation densities at the beginning of Big Ban. (iii) Dark energy is time-varying due to dynamically interacting with matter and radiation.

The cosmic fine-tuning and coincidence problems have been studied in many cosmological model extensions to  $\Lambda$ CDM, for example, quintessence [5–8], interacting dark energy model [9–19], phenomenological model [20]. People have not yet found consistent solutions to these two problems in the standard cosmology after Big Ban. In addition, these beyond  $\Lambda$ CDM scenarios have not yet given an overall consistent description of inflation, reheating, and standard cosmology epochs. In the recently proposed  $\tilde{\Lambda}$ CDM model of time-varying  $\tilde{\Lambda}$  due to dark energy and matter interactions, we describe inflation epoch [21] and reheating epoch [22]. Following these studies, in this article, we try to find and explain a self-consistent dynamical solution for the cosmic fine-tuning and coincidence problems in the standard cosmology epoch.

First, we briefly review the  $\tilde{\Lambda}$ CDM model and its applications to the inflation and reheating epoch. Then, we present the Friedman equations for the Hubble function  $H$  and time-varying dark energy  $\rho_\Lambda$ , the cosmic rate equations for matter  $\rho_M$  and radiation  $\rho_R$  densities that interact with dark energy density  $\rho_\Lambda$ . These equations form a close set of ordinary differential equations. The solution is unique, provided initial conditions are given by observations. Numerically integrating these equations, we find the  $\tilde{\Lambda}$ CDM dynamical solution: (i) in inflation and reheating, dark energy converts to matter and radiation energies and vanishes at the end of reheating; (ii) in standard cosmology, instead, matter and radiation energies convert to dark energy. The conversion rate is proportional to  $1/H$ , namely dark energy and matter interaction decreases as redshift  $z$  increases. These dynamical features yield a possible solution for the cosmic coincidence problem in  $\Lambda$ CDM. The conversion rate  $\propto 1/H$  is consistent with the late-time interaction in dark matter converting dark energy, obtained by data analysis in different  $z$  value bins [23, 24].

We compare and contrast  $\tilde{\Lambda}$ CDM with  $\Lambda$ CDM and advocate an approximate

model for phenomenological studies and data analysis. Finally, we discuss in the  $\tilde{\Lambda}$ CDM scenario the geometric and dynamic natures of  $\tilde{\Lambda}$  dark energy as a gravitational ground state, asymptotically safe Einstein theory for the early and present Universe, and  $\tilde{\Lambda}$  dark energy solution for the cosmic fine-tuning problem.

## 2 Cosmological $\tilde{\Lambda}$ CDM model

In such  $\tilde{\Lambda}$ CDM scenario, we have recently studied singularity-free and large-scale anomaly issues, the spectral index and tensor-to-scalar ratio relation in the inflation epoch [21], and calculated reheating energy and entropy [22]. The results are consistent with observations. We briefly recall three main features of the  $\tilde{\Lambda}$ CDM scenario.

### 2.1 Time-varying cosmological $\tilde{\Lambda}$ term

First, a time-varying cosmological  $\tilde{\Lambda}$  term represents interacting dark energy with matter and radiation. The Friedman equations for a flat Universe of horizon  $H$  are [25]

$$H^2 = \frac{8\pi G}{3}(\rho_M + \rho_R + \rho_\Lambda), \quad (2.1)$$

$$\dot{H} = -\frac{8\pi G}{2}(\rho_M + \rho_R + \rho_\Lambda + p_M + p_R + p_\Lambda). \quad (2.2)$$

Equations of States  $p_{M,R,\Lambda} = \omega_{M,R,\Lambda}\rho_{M,R,\Lambda}$ ,  $\omega_M = 0$  for massive particles and  $\omega_R = 1/3$  for massless radiation. The second equation of (2.2) is the generalized conservation law (Bianchi identity) for including time-varying cosmological term  $\rho_\Lambda(t) \equiv \tilde{\Lambda}(t)/(8\pi G)$  and  $\omega_\Lambda = -1$ . When  $\Lambda$  is constant in time, particles are stable, and dark energy does not interact with matter and radiation, Equation (2.2) reduces to the usual equations  $\dot{\rho}_\Lambda = 0$ ,  $\dot{\rho}_M + 3H\rho_M = 0$  and  $\dot{\rho}_R + 4H\rho_R = 0$ , whose solutions in terms of scale factor  $a$  are  $(1/a)^{3(1+\omega_{\Lambda,M,R})}$ , respectively for constant dark energy density, massive particle number and massless particle number (entropy) conservation. When interacting  $\tilde{\Lambda}$  dark energy is time-varying, Eqs. (2.1,2.2) lead to  $\dot{\rho}_\Lambda + \dot{\rho}_R + \dot{\rho}_M = -H(3\rho_R + 4\rho_M)$ , whose solutions  $\rho_{\Lambda,M,R}$  differ from the usual one. For weak  $\tilde{\Lambda}$  interacting with matter and radiation, we parameterize the solutions  $\rho_{\Lambda,M,R} \propto (1/a)^{3(1+\omega_{\Lambda,M,R}^{\text{eff}})}$  with effective equation of state  $\omega_{\Lambda,M,R}^{\text{eff}} = \omega_{\Lambda,M,R} + \delta_{\Lambda,M,R}$  and  $|\delta_{\Lambda,M,R}| \ll 1$  [37], see also Sec. 5.4. The detailed discussions are in Secs. 7 and 9 of Ref. [25].

### 2.2 Massive pair production and oscillation

Second, the spontaneous gravitational creation of massive particle and anti-particle pairs in the Friedman Universe has been intensively studied, see examples [26–28,30,34]. The massive pairs' production [26] and oscillation [21,22] establish a condensate ground state  $|\mathcal{N}_{\text{pair}}\rangle$  of the large number ( $\mathcal{N}_{\text{pair}} \gg 1$ ) and massive ( $M \gg H$ ) pairs of particles and anti-particles. They attribute to the microscopic fast-component  $H_{\text{fast}}$  in the Hubble function  $H = H_{\text{fast}} + H_{\text{slow}}$ . The fast component  $H_{\text{fast}}$  oscillates coherently with the pairs' oscillation, which relates to pairs' production and annihilation from/into the vacuum at the microscopic time scale  $1/M$ . We present in Appendix 7 the local

and fast-oscillating  $H_{\text{fast}}$  dynamics. It is consistent with recent studies of vacuum fluctuation and “microcyclic universes” at small scales, shown by local scale factor oscillation in Figure 1 of Refs. [31,32]. The macroscopic slow component  $H_{\text{slow}} \gg H_{\text{fast}}$ , and  $H_{\text{slow}} \approx H$  obeys the Friedman equation (2.2) at the “macroscopic” time scale  $1/H$ . These microscopic and macroscopic processes couple each other. However, one cannot even numerically integrate their differential equations due to the vast difference between the scale  $1/M$  and  $1/H$ . Therefore, at the macroscopic time scale  $1/H$ , averaging over microscopic states, we model the condensate ground state  $|\mathcal{N}_{\text{pair}}\rangle$  as an “equilibrium” or “equipartition” state of the microscopic fast component  $H_{\text{fast}}$  and pairs’ oscillation. It is the method that we use to study the back-reactions of microscopic fast component  $H_{\text{fast}}$  and pairs’ oscillation on macroscopic densities  $\rho_{\Lambda, M, R}$  in the Friedman equation (2.2). Detailed discussions are in Secs. 2-3 of Ref. [22].

### 2.3 Holographic and massive pair plasma state

Third, we assume the aforementioned “equilibrium” state  $|\mathcal{N}_{\text{pair}}\rangle$  is a holographic and massive pair plasma state containing a large number of massive particle and antiparticle pairs. We effectively describe such a plasma state as a perfect fluid state of effective number  $n_M^H$  and energy  $\rho_M^H$  densities of stable and unstable massive pairs,

$$\rho_M^H \equiv 2\chi m^2 H^2, \quad n_M^H \equiv \chi m H^2. \quad (2.3)$$

The equation of state and pressure are  $p_M^H = \omega_M^H \rho_M^H$ . The lower limit  $\omega_M^H \approx 0$  for  $m \gg H$ , and the upper limit  $\omega_M^H \lesssim 1/3$  for  $m \gtrsim H$ . The  $m \propto \mathcal{N}_{\text{pair}} M$  is the effective mass parameter, representing total mass and number of pairs in the massive pair plasma state (2.3). Such a state is a holographic layer near the horizon because the average of local pairs’ and  $H_{\text{fast}}$  oscillations at the scale  $1/M$  should vanish inside the horizon for global homogeneity up to the horizon, as explained in Sec. 4 of Ref. [22]. The width parameter  $\chi$  characterizes the layer radial width  $\lambda_m = (\chi m)^{-1}$ . We adopt <sup>1</sup>  $\chi = 10^{-3}$  and treat  $m$  as a free parameter. At a given horizon  $H$ , the “macroscopic” condensation state  $\rho_M^H$  (2.3) effectively represents the average overall “microscopic” states of pair production, annihilation and oscillations at the time scale  $1/M$ . Since produced pairs’ mass  $M$  and number  $\mathcal{N}_{\text{pair}}$  cannot be constant in time, we assume the effective mass parameter  $m$  weakly depends on the horizon  $H$ . Its effective value  $m_{\text{eff}}$  for each evolution epoch must be fixed by observations. The detailed discussions are in Secs. 3-4 of Ref. [22].

### 2.4 Cosmic rate equations for matter and radiation densities

Fourth, we describe how the massive pair plasma energy density  $\rho_M^H$  interacts with matter and radiation energy density  $\rho_{M, R}$ , which vary in time scale  $1/H$ . While the

---

<sup>1</sup>In Refs. [33, 34], we adopt the different renormalization prescription at high energies  $M \gg H$  from the usual prescription (subtraction) at low energies  $M \ll H$ . We have consistently obtained the mean density  $n_M^H \approx \chi m H^2$  (2.3) and  $\chi \approx 1.85 \times 10^{-3}$  by studying massive fermion pair productions in an exact De Sitter spacetime of constant  $H$  and scaling factor  $a(t) = e^{iHt}$ . This result implies  $\chi \sim \mathcal{O}(10^{-3})$ .

$\rho_M^H$  variation time scale  $\tau_M$  differs from  $1/H$  and can be estimated as follows. From the pair number density  $n_M^H$  (2.3), the total number of particles produced inside the Hubble sphere  $N \approx n_M^H H^{-3}/2$  and mean pair production rate w.r.t. macroscopic time variation  $dt$  are approximately,

$$\Gamma_M = \frac{dN}{2\pi dt} \approx \frac{\chi m}{4\pi} \epsilon, \quad \tau_M^{-1} = \Gamma_M. \quad (2.4)$$

The Universe evolution  $\epsilon$ -rate is usually defined as,

$$\epsilon \equiv -\frac{\dot{H}}{H^2} = \frac{3}{2} \frac{(1 + \omega_M)\rho_M + (1 + \omega_R)\rho_R + (1 + \omega_\Lambda)\rho_\Lambda}{\rho_\Lambda + \rho_M + \rho_R}, \quad (2.5)$$

where the second equality comes from the Friedman equations (2.2). The asymptotic values  $\epsilon \ll 1$ ,  $\epsilon \approx 2$ , and  $\epsilon \approx 3/2$  correspond to dark energy, radiation, and matter domination, respectively.

The massive pair plasma state density  $\rho_M^H$  associated with the horizon contributes to the matter/radiation density  $\rho_{M,R}$  in Friedman equations (2.1) and (2.2). In turn, the  $\rho_{M,R}$  variation affects the  $\rho_M^H$  via the horizon  $H$ . It implies the back-and-forth interaction between the massive pair plasma state and the matter/radiation state during the Universe's evolution. Moreover, the massive pair plasma state  $\rho_M^H$  (2.3) has a microscopic ‘‘relaxation’’ time scale  $\tau_M = \Gamma_M^{-1}$  (2.4), differing from the macroscopic one  $\tau_H = H^{-1}$  of the matter/radiation state  $\rho_{M,R}$  in Friedman equations (2.1) and (2.2), i.e.,  $\tau_H \gg \tau_M$ . Therefore, we cannot simply add  $\rho_M^H$  into  $\rho_{M,R}$  in Friedman equations.

By analogy with the rate equation for a microscopic back-and-forth process, e.g.,  $e^+e^- \leftrightarrow \gamma\gamma$ , in macroscopic expansion (see part of Eq. (5.4) in Ref. [22]), we propose the back-and-forth interaction between the densities  $\rho_M^H$  and  $\rho_{M,R}$  follows the cosmic rate equations of Boltzmann type,

$$\dot{\rho}_M + 3(1 + \omega_M)H\rho_M = \Gamma_M(\rho_M^H - \rho_M - \rho_R) - \Gamma_M^{\text{de}}\rho_M^{\text{de}}, \quad (2.6)$$

$$\dot{\rho}_R + 3(1 + \omega_R)H\rho_R = \Gamma_M(\rho_M^H - \rho_M - \rho_R) + \Gamma_M^{\text{de}}\rho_M^{\text{de}}. \quad (2.7)$$

The term  $3(1 + \omega_{M,R})H\rho_{M,R}$  of the time scale  $[3(1 + \omega_{M,R})H]^{-1}$  represents the space-time expanding effect on the density  $\rho_{M,R}$ . The detailed balance term  $\Gamma_M(\rho_M^H - \rho_M - \rho_R)$  indicates how densities  $\rho_M^H$  and  $\rho_{M,R}$  of different time scales couple together in back-and-forth interaction.  $\Gamma_M\rho_M^H$  is the source term, indicating  $\rho_M^H$  contribution to increasing  $\rho_{M,R}$ .  $\Gamma_M(\rho_M + \rho_R)$  is the depletion term, indicating back reaction reducing  $\rho_{M,R}$ . The ratio  $\Gamma_M/H > 1$  indicates the coupled case, and  $\Gamma_M/H < 1$  indicates the decoupled case. There are unstable massive pairs of density  $\rho_M^{\text{de}}$  inside the massive pair plasma state (2.3). The term  $\Gamma_M^{\text{de}}\rho_M^{\text{de}}$  represents unstable massive pairs decay to light particles, such as quarks and leptons, gauge bosons in SM and other light sterile particles. The detailed discussions are in Secs. 4-5 of Ref. [22].

## 2.5 Preliminary applications to inflation and reheating

The main aspects of the  $\tilde{\Lambda}$ CDM scenario are (a) the dark energy and matter interacting Friedman Equations (2.1,2.2); (b) massive particle and antiparticle pairs' production

and oscillation; (c) a holographic massive pair plasma state (2.3) and its variation rate (2.4); (d) cosmic rate equations (2.6) and (2.7). They form a close set of first-order ordinary differential equations for the densities  $\rho_M, \rho_R, \rho_\Lambda$  and Hubble function  $H$ . The solutions are completely determined, provided initial or transition conditions and effective mass parameter  $m_{\text{eff}}$  are fixed by observations.

In Ref. [21], we study the inflation when the dominant dark energy  $\rho_\Lambda$  drives inflation and produces massive pairs' plasma  $\rho_M^H$ , that contributes to the matter  $\rho_M$  and slows down inflation ( $\rho_\Lambda \gg \rho_M^H \approx \rho_M$ ). Neglecting Eqs. (2.6,2.7) for the decoupled case  $\Gamma_M/H < 1$ , we approximately use Eq. (2.2) and  $\rho_M \approx \rho_M^H$  to obtain an analytical solution  $H_{\text{end}} = H_* \exp(-\epsilon^* N_{\text{end}})$ . The  $e$ -folding numbers  $N_{\text{end}} \approx (50-60)$  from the CMB pivot scale  $H_*$  to the inflation end  $H_{\text{end}} \approx \Gamma_M \approx (0.42, 0.35)H_*$ . In the inflation epoch, we fix the effective value of mass parameter  $m_{\text{eff}} = m_*$  by  $\epsilon^* = \chi(m_*/m_{\text{pl}})^2 = (1 - n_s)/2$ <sup>2</sup>. The obtained relation of spectral index  $n_s$  and tensor-to-scalar ratio  $r$  agrees with recent CMB observations. We discuss the singularity-free pre-inflation, the CMB large-scale anomaly, and dark-matter density perturbations imprinting on power spectra.

In Ref. [22], we study the reheating when the dark energy  $\rho_\Lambda$  decreases,  $\rho_M^H$  and  $\rho_M$  increase. The competition between the Hubble function  $H$ , the massive pair plasma variation rate  $\Gamma_M$  (2.4) and massive pairs' decay rate  $\Gamma_M^{\text{de}}$  play an important role in cosmic rate equations (2.6) and (2.7). First, it appears the  $\mathcal{M}$ -episode of massive pair domination when  $\Gamma_M > H > \Gamma_M^{\text{de}}$ . Then it proceeds to the  $\mathcal{R}$ -episode of radiation domination when  $\Gamma_M^{\text{de}} > H > \Gamma_M$ . The cosmic rate equation (2.7) becomes a reheating equation for  $\Gamma_M^{\text{de}} > \Gamma_M$ . Unstable pairs decay to light particles, and the radiation energy  $\rho_R$  increases, leading to reheating. In the reheating epoch, we fix the effective value of mass parameter  $m_{\text{eff}} = \hat{m} \gtrsim 20 m_{\text{pl}}$  and obtained results agree with observations. Stable massive particles remain as cold dark matter particles<sup>3</sup>. The detailed discussions are in Secs. 7.2-7.3 of Ref. [22].

### 3 $\tilde{\Lambda}$ CDM equations of dark energy and matter interaction

At the reheating end, the radiation energy density  $\rho_R$  is dominant, stable cold dark matter energy density  $\rho_M \ll \rho_R$  and the dark energy density nearly vanishes  $\rho_\Lambda \approx 0$ , namely  $\rho_R \gg \rho_M \gg \rho_\Lambda \approx 0$ . These are the initial conditions starting the standard cosmology. It then evolves to matter-dominated, dark energy-dominated epochs. We study in this article the  $\tilde{\Lambda}$ CDM equation and solution after reheating, focusing on the problem of cosmological coincidence between dark energy and matter.

<sup>2</sup>The reduced Planck mass  $m_{\text{pl}} \equiv (8\pi)^{-1/2} M_{\text{pl}} = 2.43 \times 10^{18} \text{GeV}$ .

<sup>3</sup>There, the strongly coupled case  $\Gamma_M/H \gg 1$  is assumed in the preliminary study of cold dark matter abundance  $\Omega_M$  evolution. We realise it should be the weakly coupled case  $\Gamma_M/H < 1$  after studying the  $\Omega_M$  evolution in this article.

### 3.1 Dark energy interaction with matter and radiation

To explicitly show dark energy and matter interaction, we recast the Friedman equations (2.1,2.2), cosmic rate equations (2.6) and (2.7) as

$$\dot{\rho}_\Lambda + 3(1 + \omega_\Lambda)H\rho_\Lambda = -2\Gamma_M(\rho_M^H - \rho_M - \rho_R), \quad (3.1)$$

$$\dot{\rho}_M + 3(1 + \omega_M)H\rho_M = +\Gamma_M(\rho_M^H - \rho_M - \rho_R), \quad (3.2)$$

$$\dot{\rho}_R + 3(1 + \omega_R)H\rho_R = +\Gamma_M(\rho_M^H - \rho_M - \rho_R), \quad (3.3)$$

where  $\Gamma_M(\rho_M^H - \rho_M - \rho_R)$  represents the interaction between dark energy and matter/radiation via the massive pair plasma state  $\rho_M^H$ . Equations (3.2) and (3.3) are the cosmic rate equations (2.6) and (2.7). Here we neglect the decay term  $\pm\Gamma_M^{\text{de}}\rho_M^{\text{de}}$  in Eqs. (2.6,2.7), assuming unstable massive pairs  $\rho_M^{\text{de}}$  have decayed in reheating. The dark-energy equation (3.1) is derived from the generalized Friedman equation (2.2) by using cosmic rate equations (3.2) and (3.3). It shows the dark energy interacting with matter and radiation via the back-and-forth balance term  $\Gamma_M(\rho_M^H - \rho_M - \rho_R)$ , massive pair plasma state  $\rho_M^H$  (2.3) and interacting rate  $\Gamma_M$  (2.4).

During inflation and reheating epochs, the balance term  $\Gamma_M(\rho_M^H - \rho_M - \rho_R)$  is positive in dark energy equation (3.1) and cosmic rate equations (3.2,3.3). As results,  $\dot{\rho}_\Lambda < 0$  and  $\dot{\rho}_{M,R} > 0$ , namely dark energy converts to matter and radiation energies [21,22]. During standard cosmology epoch after reheating, two cases are possible:

- (a) negative detailed balance term  $\rho_M^H < \rho_M + \rho_R$ , matter and radiation converts to dark energy  $\dot{\rho}_\Lambda > 0$ ,
- (b) positive detailed balance term  $\rho_M^H > \rho_M + \rho_R$ , dark energy converts to matter and radiation  $\dot{\rho}_\Lambda < 0$ .

These two cases are separated by  $\rho_M + \rho_R = \rho_M^H$ .

### 3.2 A close set of ordinary differential equations for cosmic abundance

We define cosmic abundance

$$\Omega_{\Lambda,M,R} \equiv \frac{\rho_{\Lambda,M,R}}{\rho_{\text{tot}}}, \quad \rho_{\text{tot}} \equiv \frac{3}{8\pi G}H^2, \quad (3.4)$$

and  $\Omega_\Lambda + \Omega_M + \Omega_R = 1$  (2.1). The ‘‘time’’ variable  $x$  relates to the scale factor  $a = a(t)$ ,

$$x = \ln(a/a_0) + \ln(a_0/a_R) = -\ln(1+z) + \ln(a_0/a_R). \quad (3.5)$$

The derivative  $dx = Hdt$  and  $dx = -dz/(1+z)$ , where  $z$  is the redshift. Equation (2.5) becomes

$$\epsilon = (1+z)\frac{dH}{Hdz} = \frac{3}{2} [(1+\omega_M)\Omega_M + (1+\omega_R)\Omega_R + (1+\omega_\Lambda)\Omega_\Lambda]. \quad (3.6)$$



Whereas, Equations (3.1-3.3) becomes

$$-(1+z)\frac{d\Omega_\Lambda}{dz} + 3(1+\omega_\Lambda)\Omega_\Lambda = -2\frac{\Gamma_M}{H}(\Omega_M^H - \Omega_M - \Omega_R), \quad (3.7)$$

$$-(1+z)\frac{d\Omega_M}{dz} + 3(1+\omega_M)\Omega_M = +\frac{\Gamma_M}{H}(\Omega_M^H - \Omega_M - \Omega_R), \quad (3.8)$$

$$-(1+z)\frac{d\Omega_R}{dz} + 3(1+\omega_R)\Omega_R = +\frac{\Gamma_M}{H}(\Omega_M^H - \Omega_M - \Omega_R), \quad (3.9)$$

where  $\Omega_M^H = (2/3)\chi(\bar{m}/M_{\text{pl}})^2$  and the  $\bar{m}$  represents the effective mass parameter value  $m_{\text{eff}} = \bar{m}$  after reheating. The dark energy and matter interacting rate  $\Gamma_M/H$  is characterized by the ratio

$$\frac{\Gamma_M}{H} = \frac{\chi\epsilon}{(4\pi)} \frac{(\bar{m}/H_0)}{(H/H_0)}, \quad (3.10)$$

and  $H_0$  is the Hubble constant at the present time  $a_0 = 1$  and  $z_0 = 0$ . We define the dark energy and matter exchanging amount  $\delta Q$

$$\delta Q \equiv \frac{\Gamma_M}{H}(\Omega_M^H - \Omega_M - \Omega_R). \quad (3.11)$$

Both rate  $\Gamma_M/H$  and amount  $\delta Q$  are functions of redshift  $z$ . These equations are nonlinear, and  $\Omega_{\Lambda,M,R}$  and  $H$  couple together.

### 3.3 Initial condition at present or reheating time

The ordinary differential equations (3.7,3.8,3.9) and condition  $\Omega_\Lambda + \Omega_M + \Omega_R = 1$  form a closed set. Its solutions  $\Omega_{\Lambda,M,R}(z)$  and  $H(z)$  are unique, provided the initial values  $\Omega_{\Lambda,M,R}(z_i)$  and  $H(z_i)$  are given by measurements at a redshift  $z_i$ . The uniqueness states that the solutions  $\Omega_{\Lambda,M,R}(z)$  and  $H(z)$  do not depend on the redshift  $z_i$  where we implement the initial values. We consider initial values at two particular redshifts.

- (i) The initial values given by observations today ( $a_0 = 1$  and  $z_0(a_0) = 0$ )

$$\Omega_\Lambda^0 \approx 0.7, \quad \Omega_M^0 \approx 0.3, \quad \Omega_R^0 \approx 3 \times 10^{-5}, \quad (3.12)$$

and  $H_0$ . The first-order ordinary differential equations (3.6-3.9) determine the solutions  $\Omega_\Lambda, \Omega_M, \Omega_R$  and  $H$  as functions of the redshift  $z$ , varying from the today  $z_0 = 0$  to the past  $z_R$  of the reheating end, and to the future  $z \rightarrow -1$ .

- (ii) The initial values  $\Omega_{R,M,\Lambda}(z_R)$  and  $H(z_R)$  are given at the reheating end  $a_R$  and

$$(1+z_R) = a_0/a_R \approx (g_*/2)^{1/3}(T_{\text{RH}}/T_{\text{CMB}}). \quad (3.13)$$

The first-order ordinary differential equations (3.6-3.9) also determine the solutions  $\Omega_\Lambda, \Omega_M, \Omega_R$  and  $H$  as functions of the redshift  $z$ , varying from the reheating end  $z_R$  to the today  $z_0 = 0$ , and to the future  $z \rightarrow -1$ .

The solution we obtain by using the initial values at  $z_0$  must be identical to the one we obtain by using the initial values at  $z_R$ . The question is that we do not know values  $z_R$ ,  $\Omega_{R,M,\Lambda}(z_R)$  and  $H(z_R)$  at the reheating end  $z_R$  (3.13), which depends on the degeneracy  $g^*$  of relativistic particles, the reheating temperature  $T_{\text{RH}}$  and CMB temperature  $T_{\text{CMB}}$  [22, 35]. However, we do know the  $z_R \gg 1$  for  $T_{\text{RH}} \gg T_{\text{CMB}}$ , and the Hubble scale  $H(z_R) = H_{\text{RH}} \sim T_{\text{RH}} \gg H_0$ .

## 4 Cosmological coincidence problem

In the  $\Lambda$ CDM model, dark energy density  $\rho_\Lambda = \Lambda/(8\pi G)$  and  $\omega_\Lambda = -1$  are constant in time, decoupling from matter and radiation. This is the case  $\Gamma_M \equiv 0$  in Eqs. (3.7,3.8,3.9). The ratio of dark energy and matter-radiation components is

$$\frac{\rho_\Lambda}{\rho_R + \rho_M} = \frac{\Omega_\Lambda}{\Omega_R + \Omega_M} \xrightarrow{\Lambda\text{CDM}} \frac{\Omega_\Lambda^0}{\Omega_R^0 + \Omega_M^0} \left(\frac{a}{a_0}\right)^{3\sim 4}, \quad (4.1)$$

which becomes

$$\frac{\Omega_\Lambda}{1 - \Omega_\Lambda} \approx \Omega_\Lambda \xrightarrow{\Lambda\text{CDM}} 2.33 \left(\frac{a}{a_0}\right)^{3\sim 4}. \quad (4.2)$$

It shows that at the reheating end  $a = a_R \ll a_0$  and  $z_R + 1 = (a_0/a_R) \gg 1$ , the tiny value  $\Lambda \gtrsim 0$  or  $\rho_\Lambda \gtrsim 0$  must be extremely unnaturally fine-tuned many orders of magnitudes to achieve the present ratio 2.33 of dark energy and matter-radiation densities. It is the cosmological coincidence problem of the  $\Lambda$ CDM, which is caused by (i)  $\Lambda$  being a free parameter in usual Friedman equations and (ii)  $\rho_\Lambda$  being a constant whereas  $\rho_{R,M} \propto a^{-(3\sim 4)}$  decreasing in a very long period of evolution.

In the  $\tilde{\Lambda}$ CDM model, basic Eqs. (3.1,3.8,3.9) and initial values (3.12) have uniquely determined the solutions of coupled dark energy and matter-radiation densities and their ratio (4.1). Likewise, matter/radiation density  $\rho_{M,R}$ , the dark energy  $\rho_\Lambda$  or  $\tilde{\Lambda}$  is a dynamical solution, rather than a free parameter for fine-tuning. However, the issues we need to investigate are

- (i) whether or not  $\tilde{\Lambda}$ CDM nonlinear Eqs. (3.1,3.8,3.9) give physical solutions with sensible value  $\tilde{m}/H_0$ , which evolve in time from the present values (3.12) to the reheating values

$$\Omega_R \gg \Omega_M \gg \Omega_\Lambda \quad \text{i.e.,} \quad \rho_R \gg \rho_M \gg \rho_\Lambda, \quad (4.3)$$

or the equivalent inverse evolution from the reheating end (4.3) to today (3.12). Namely, it is the unique solutions to Eqs. (3.7-3.9) with boundary conditions (3.12) and (4.3).

- (ii) we should obtain such unique solutions without fine-tuning the effective mass parameter  $\tilde{m}/H_0$ ;

- (iii) if such solutions exist, how the solutions evolve in an extremely long period after the reheating and achieve the present values (3.12).

Comparing and contrasting with  $\Lambda$ CDM, we will show how  $\tilde{\Lambda}$ CDM solutions possibly evade the cosmological coincidence problem.

#### 4.1 Unique solution to $\tilde{\Lambda}$ CDM equations and boundary conditions

The Hubble scale  $H$  and scale factor  $a$  variations are huge after reheating. The Universe evolves through radiation-, matter- and dark-energy-dominated epochs. The effective values of the mass parameter  $\bar{m}$  can be different in different epochs. In this article, we study a possible solution to the cosmological coincidence problem, rather than a quantitative analysis of a specific epoch of the Universe. Therefore, we treat the mass parameter  $\bar{m}/H_0 > 1$  as an effective mean value for qualitatively studying  $\Omega_\Lambda$ ,  $\Omega_M$ ,  $\Omega_R$  and  $H$  evolution. The value  $\bar{m}/H_0$  should be fixed by observation data.

We present the numerical solutions in Figure 1, the left column for the future  $0 > z > -1$  and the right column for the past  $z_R > z > 0$ . This solution is unique and independent of where the initial condition  $z = 0$  or  $z = z_R$  is implemented. We have numerically checked the uniqueness of the solution. Using the initial values (3.12), we obtain the solution and the final values at  $z_R$ . As a check, using the final values at  $z_R$  as the initial values, we resolve the different equations (3.7,3.8,3.9) to achieve the values (3.12) at  $z_0 = 0$ .

We first figure out the novel features of the  $\tilde{\Lambda}$ CDM solution, compared and contrasted with the  $\Lambda$ CDM. The discussions on the numerical solution are in order:

- (i) Figures 1 (a) and (b) show  $\Omega_{R,M,\Lambda}$  evolution in time (or inverse time): (a) from the today  $z = 0$  (3.12) to the future ( $z = -1$ ) when  $\Omega_R \rightarrow 0, \Omega_M \rightarrow 0$  and  $\Omega_\Lambda \rightarrow 1$ ; (b) from  $z \approx z_R$  radiation domination  $\Omega_R \approx 1, \Omega_M \ll 1$  and  $\Omega_\Lambda \approx 0$  to the today  $z = 0$  (3.12). From  $z = z_R$  to  $z = 0$ , the matter increases, radiation decreases and  $\Omega_R = \Omega_M$  occurs around  $z \sim (10^3 - 10^4)$  for the effective mass parameter  $\bar{m}/H_0 \sim (5 - 10)$ . The equality  $\Omega_\Lambda = \Omega_M$  occurs around  $z \approx 0.2 \sim 0.4$ , which is not sensitive to the parameter  $\bar{m}/H_0$  value. Figures 1 (c) and (d) show the Universe evolution  $\epsilon$  rate (2.5) varies from  $\epsilon \approx 2$  (radiation) to  $\epsilon \approx 3/2$  (matter),  $\epsilon \approx 0.45$  (today), and then to  $\epsilon \approx 0$  (dark energy) domination. The quantitative results mildly depend on the parameter value  $\bar{m}/H_0$ . All these behaviors qualitatively but not quantitatively follow the  $\Lambda$ CDM model, as shown and explained later.
- (ii) Figures 1 (e) and (f) show the solution of how the Hubble function in the unit of  $H_0$  evolves from  $z = z_R$  to  $z = 0$  then to  $z = -1$ . The approximate constancy  $H \approx H_0$  since  $z \approx 0.1$  shows the Universe acceleration and dark energy  $\Omega_\Lambda$  domination over matter  $\Omega_M$  and radiation  $\Omega_R$ . Towards the future  $z < 0$ ,  $H^2 \approx (8\pi/3)G\rho_\Lambda$  slowly varies, asymptotically approaching to constant  $\Omega_\Lambda \lesssim 1$ . The evolution is analogous to inflation.
- (iii) Figures 1 (g) and (h) show the dark energy and matter interacting rate  $\Gamma_M/H$  is small and exchanging amount  $\delta Q$  (3.11) is negative. Therefore, the matter

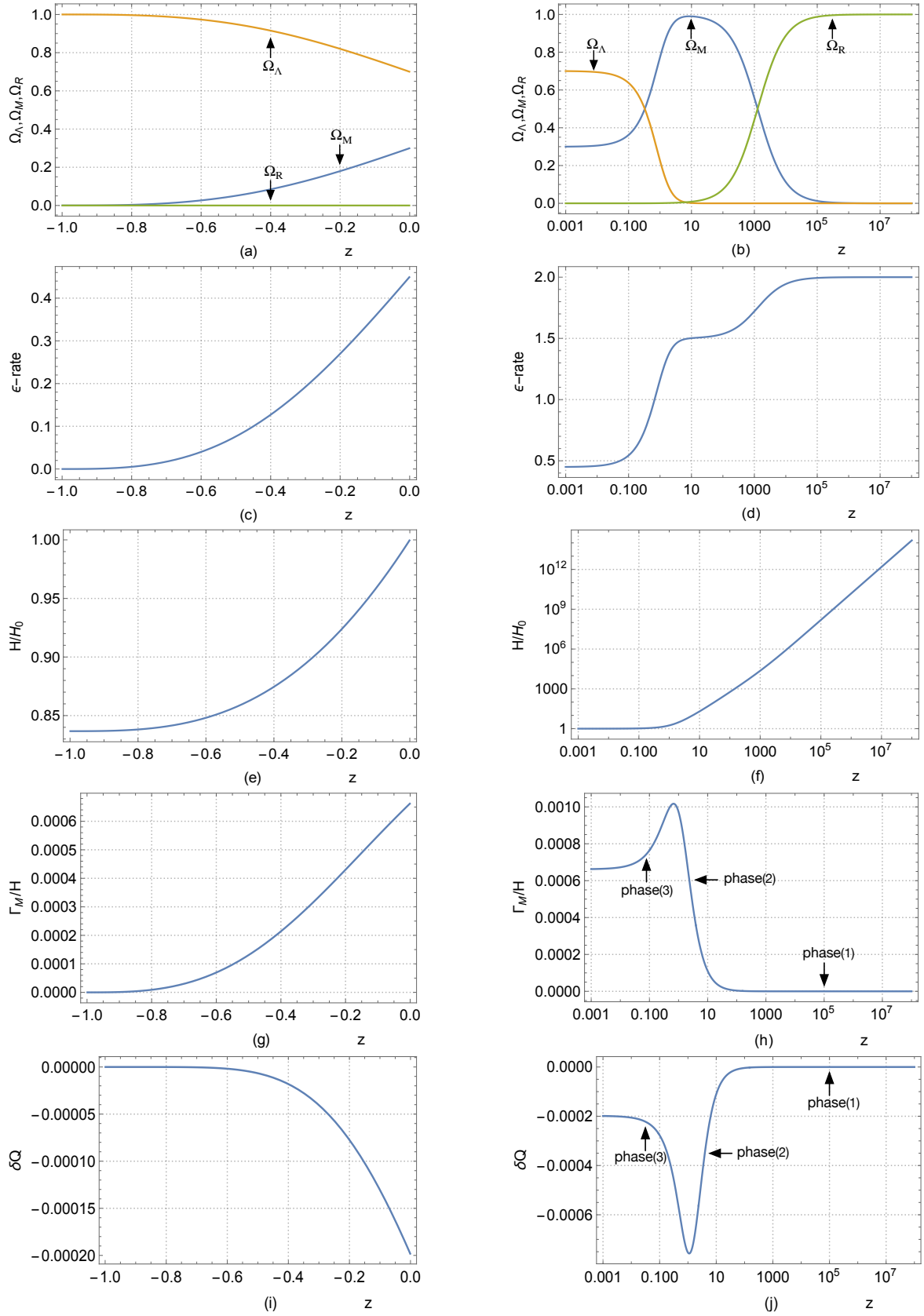


**Figure 1.** Numerically solving Eqs. (3.6-3.9) and (3.12),  $\bar{m}/H_0 = 10$ , we present the  $\tilde{\Lambda}$ QCD solutions as functions of redshift  $z$  from today to the future (the left column) and to the past (the right column). See text for detailed discussions.

and radiation energy slowly convert to the dark energy from the reheating end  $z = z_R$  to today  $z = 0$ , then to the future  $0 > z > -1$ . The dark energy  $\Omega_\Lambda(z)$  increases from  $\Omega_\Lambda(z_R) \approx 0$  to  $\Omega_\Lambda(0) \approx 0.7$  and then to  $\Omega_\Lambda(-1) \approx 1$ . For values  $\bar{m} \sim (5 \sim 10)H_0$  and  $H_0 \ll M_{\text{pl}}$ , we can neglect the  $\Omega_M^H = (2/3)\chi(\bar{m}/M_{\text{pl}})^2 \ll 1$ , and the  $\bar{m}/H_0$  is a unique parameter for differential equations (3.7-3.9).

We have made numerical verification that the  $\tilde{\Lambda}$ CDM solution from the maximal  $\Omega_M$  ( $z \approx 5$ ) to  $\Omega_M \approx \Omega_\Lambda$  ( $z \approx 0.5$ ) does not sensitively depend on the effective value of mass parameter  $\bar{m}/H_0$ . It implies that the  $\tilde{\Lambda}$ CDM solution should not qualitatively change its behaviour, if we adopt the mass parameter  $\bar{m}$  weakly depending on  $H$ .

To end this section, we mention that in the remote future ( $z \rightarrow -1$ ) of dominant dark energy, radiation and matter  $\Omega_R + \Omega_M$  continually decrease until the exchanging amount  $\delta Q$  (3.11) changes sign from negative  $\delta Q < 0$  to positive  $\delta Q > 0$ . The dark energy density decreases, converting to matter and radiation energy densities. It shows the possibility that the Universe ends the current acceleration and starts recycling again. The topic is not the scope of this article. We do not present figures and discussions for this situation in the remote future  $z \rightarrow -1$ .

## 4.2 Three evolution phases evading cosmological coincidence problem

The novelty is that the  $\tilde{\Lambda}$ CDM results of Fig. 1 show a natural solution to the cosmic coincidence problem of the  $\Lambda$ CDM model. We explain below how the solution works. The results show that the dark energy density almost vanishes ( $\rho_\Lambda \gtrsim 0$ ) at the reheating end  $z_R$  and undergoes three evolution phases to achieve its value today.

*The phase (1):* for a long period ( $10 \lesssim z \lesssim z_R$ ), it slowly increases ( $\rho_\Lambda \gtrsim 0$ ) and closely follows up with radiation  $\rho_R$  and matter energy  $\rho_M$  densities' evolution, see Figures 1 (b) and 2 (c) for large  $z \gtrsim 10$ . The reason is that the dark-energy, matter, and radiation interacting rate  $\Gamma_M/H \ll 1$  and exchanging amount  $\delta Q \ll 1$  are very small, but not zero, see Figure 1 (h) and (j). It is crucial for the dark energy density  $\rho_\Lambda$  following up the energy densities  $\rho_R$  and  $\rho_M$  since they had been varying many orders of magnitudes in the  $10 \lesssim z \lesssim z_R$  period. This phase is absent in  $\Lambda$ CDM<sup>4</sup>.

*The phase (2):* when the redshift  $z \lesssim 10$ , the interacting rate  $\Gamma_M/H$  and exchanging amount  $\delta Q < 0$  increase significantly because the Hubble function  $H$  becomes smaller and smaller, see Figure 1 (h) and (j). The dark energy significantly increases around  $z \approx 5$  when the matter  $\Omega_M$  domination begins<sup>5</sup>, see Fig. 1 (b). These features are consistent with the late-time interaction in the dark sector observed by data analysis [23]. As a result, in a short period from  $z \approx 5$  to  $z \approx 0.5$ , dark energy  $\Omega_\Lambda$  increases from  $\Omega_\Lambda \ll 1$  to the order of unit  $\mathcal{O}(1)$ . The  $\Omega_\Lambda$  and  $\Omega_M$  coincide  $\Omega_\Lambda \approx \Omega_M$  at  $z \approx 0.5$ . They are in the same order of magnitude up to  $z \gtrsim 0$ . In this short period  $0.5 \lesssim z \lesssim 5$ , the energy densities  $\rho_M$  and  $\rho_R$ , and Hubble function  $H$  vary only a few orders of magnitudes, see Fig. 1 (b) and (h), in contrast with their variations in many orders of magnitudes in the long period  $10 \lesssim z \lesssim z_R$  of the phase (1). In other words,

<sup>4</sup>It is a very long period, which is why the  $\Lambda$ CDM has a fine-tuning problem.

<sup>5</sup>This is consistent with the discussions that dark energy evolution follows first radiation then matter in different ways [33,34].

the low-redshift  $\rho_M$  and  $\rho_\Lambda$  evolution are insensible to their initial values at  $z_R$ . Nature does not need to fine-tune the initial ratios of dark energy, matter and radiation densities at the Big Bang beginning (the reheating end) to achieve  $\rho_\Lambda/(\rho_M + \rho_R) \sim \mathcal{O}(10^0)$  today. This phase is absent in the  $\Lambda$ CDM.

*The phase (3):* In the period  $0 \lesssim z \lesssim 0.5$ , the dark energy  $\Omega_\Lambda$ , matter and radiation  $\Omega_{M,R}$  approach their values today. The  $\Lambda$ CDM has similar behaviours in this phase. As will be shown, the  $\Lambda$ CDM and  $\tilde{\Lambda}$ CDM solutions qualitatively agree with each other.

These three distinct phases (1), (2), and (3) attribute to the properties that the dark energy, matter, and radiation interacting rate  $\Gamma_M/H$  (3.10) and exchanging amount  $\delta Q < 0$  (3.11) are small at high redshift  $z$ , and large at low redshift  $z$ . The phase (2) ( $z \approx 0.5 \sim 10$ ) separates the phase (3) ( $z \approx 0 \sim 0.5$ ) from the phase (1) ( $z \approx 10 \sim z_R$ ). Due to such a redshift  $z$  dependence of the interaction,  $\tilde{\Lambda}$ CDM evades the problem of fine-tuning  $\rho_\Lambda$  value at the reheating end to achieve its present value  $\rho_\Lambda^0$ . In other words, it gives a dynamical solution to the cosmic coincidence problem of  $\Lambda$ CDM without fine-tuning on  $\bar{m}/H_0$ . The  $\tilde{\Lambda}$ CDM dynamical solution uniquely determines the evolution from today  $\Omega_M(0) \sim \Omega_\Lambda(0) \gg \Omega_R(0)$  to the reheating end  $\Omega_R(z_R) \gg \Omega_M(z_R) \gg \Omega_\Lambda(z_R) \approx 0$ , and *vice versa*. Namely, if we would know the initial conditions  $\Omega_{R,M,\Lambda}(z_R)$  at  $z \approx z_R$  (3.13), we would have obtained the same dynamical solutions (Fig. 1) and the present values (3.12) without fine-tuning.

To indicate the  $\rho_\Lambda$  increase following up  $\rho_{R,M}$  evolution in three phases, we here adopt the word “following-up” solution, which has a similar sense as the word “tracker” solution used in Ref. [2]. However, the two solutions are different, which we will discuss in Sec. 5.3.

We do not discuss the dark energy density perturbations ( $\delta\rho_\Lambda, \delta p_\Lambda$ ) caused by its time-varying interaction with matter and radiation. However, we speculate that dark energy undergoes transitions and becomes dominant from  $z \approx 5$  to  $z \approx 0.1$  should impact matter density perturbation, leading to the effect on the formation of large-scale structures and clusters. In addition, it should induce the peculiar fluctuations of the gravitational field, possibly imprinting on observations, for instance, the integrated Sachs-Wolfe effect or galaxy positions. The reason is that the dark energy  $\Lambda$  results on the gravitation field are very different from the gravitational potential of matter.

## 5 Comparison and contrast with $\Lambda$ CDM and other models

In this section, we present the  $\tilde{\Lambda}$ CDM solutions in comparison and contrast with the  $\Lambda$ CDM solutions, other dark-energy interacting model solutions, and tracker solutions for cosmic coincidence.

### 5.1 Contrast with $\Lambda$ CDM solutions

In the  $\Lambda$ CDM model, we define the cosmic abundance of radiation, matter, and dark energy

$$\Omega_R = \Omega_R^0 \frac{(1+z)^4}{E(z)^2}, \quad \Omega_M = \Omega_M^0 \frac{(1+z)^3}{E(z)^2}, \quad \Omega_\Lambda = \Omega_\Lambda^0 \frac{(1+z)^0}{E(z)^2}, \quad (5.1)$$

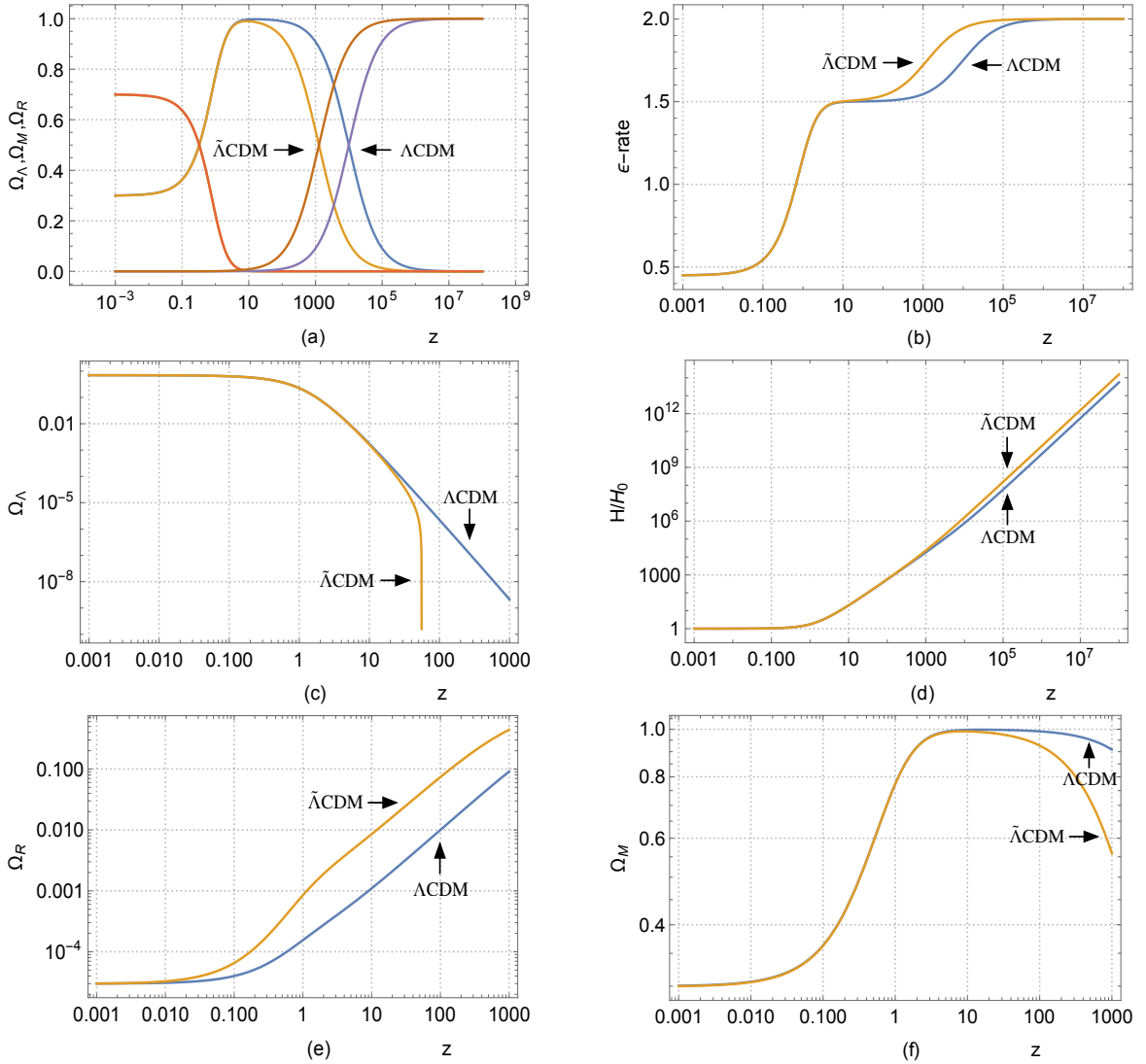


**Figure 2.** We present the  $\tilde{\Lambda}$ CDM solutions (orange) in comparison and contrast with the canonical  $\Lambda$ CDM solutions (blue) of Eqs. (5.1), (5.2) and (3.12). See text for detailed discussions.

and the dimensionless Hubble function  $E(z) \equiv (H/H_0)$

$$E(z)^2 = \Omega_R^0(1+z)^4 + \Omega_M^0(1+z)^3 + \Omega_\Lambda^0(1+z)^0, \quad (5.2)$$

where  $E(0)^2 = \Omega_R^0 + \Omega_M^0 + \Omega_\Lambda^0 = 1$ . The evolution  $\epsilon$ -rate is given by Eq. (3.6). The values  $\Omega_R^0, \Omega_M^0, \Omega_\Lambda^0$  and  $\dot{H}_0$  at  $z = 0$  are the same as the initial conditions (3.12). Here we use the same notations for quantities of the  $\tilde{\Lambda}$ CDM and  $\Lambda$ CDM models. The former is the dark energy and matter interacting solutions to Eqs. (3.6-3.9). The latter is (5.1) and (5.2) for the constant dark energy density. We have implemented only one observed data point (3.12) for both models.

In Figs. 2 and 3, we compare  $\tilde{\Lambda}$ CDM solutions (Fig. 1) with the  $\Lambda$ CDM (5.1-5.2) results. The discussions are in order.

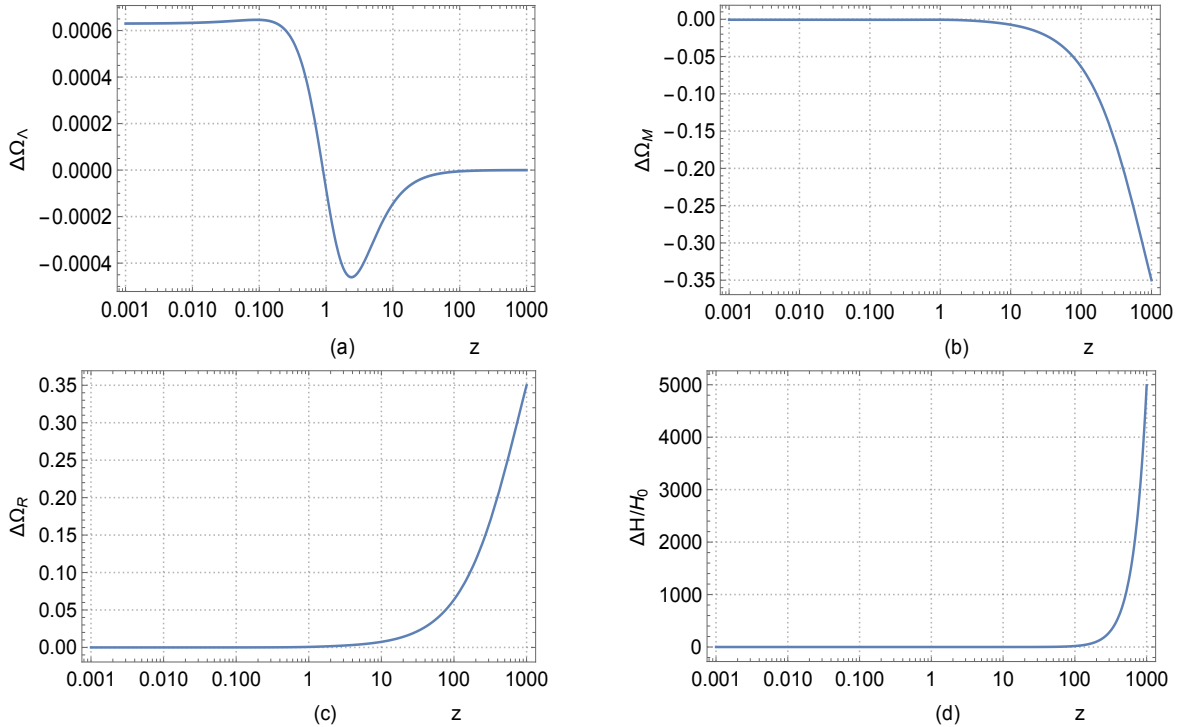


**Figure 3.** We present the quantitative differences (5.3) between  $\tilde{\Lambda}$ CDM (3.12) and  $\Lambda$ CDM models (5.1). See text for detailed discussions.

- (i) Figures 2 (a) and (b) show  $\Omega_{R,M,\Lambda}$  and expansion rate  $\epsilon$  (3.6) evolution for  $\Lambda$ CDM and  $\tilde{\Lambda}$ CDM. Overall, they are consistent and qualitatively agree with each other for  $z < 10$ . Two  $\Omega_\Lambda$  curves overlap in (a), and the point  $\Omega_\Lambda = \Omega_M$  is about the same, but quantitative numbers are different. The main differences are (i) the  $\epsilon$ -rate are in the range  $z \sim 10^2 \sim 10^5$ , (ii) the crossing point  $\Omega_R = \Omega_M$ , and (iii)  $\Omega_{R,M,\Lambda}$  in large redshift  $z > 10$ , see Figs. 2 (c), (e), and (f). We show in Fig. 3 the quantitative differences

$$\begin{aligned} \Delta\Omega_{\Lambda,M,R} &= \Omega_{\Lambda,M,R}|_{\tilde{\Lambda}\text{CDM}} - \Omega_{\Lambda,M,R}|_{\Lambda\text{CDM}}, \\ \Delta(H/H_0) &= (H/H_0)|_{\tilde{\Lambda}\text{CDM}} - (H/H_0)|_{\Lambda\text{CDM}} \end{aligned} \quad (5.3)$$

between  $\tilde{\Lambda}$ CDM and  $\Lambda$ CDM. We have made numerical checks and found these differences mildly depend on the  $\tilde{\Lambda}$ CDM parameter value  $\tilde{m}/H_0$  in the range  $\mathcal{O}(10^1) \sim \mathcal{O}(10^2)$ .

- (ii) Figures 2 (d), (e), and (f) show  $H/H_0$ ,  $\Omega_R$  and  $\Omega_M$  evolution for  $\tilde{\Lambda}$ CDM and  $\Lambda$ CDM. Figures 3 (b), (c), and (d) show the differences between the two models. The discrepancies between  $\tilde{\Lambda}$ CDM and  $\Lambda$ CDM are significant at high red-shift ( $z > 10^2$ ). These comparisons and contrasts imply that the  $\tilde{\Lambda}$ CDM could relieve the  $H_0$  and  $S_8$  tensions between the values measured today and values calculated in the  $\Lambda$ CDM model based on measurements at high red-shifts  $z$ .



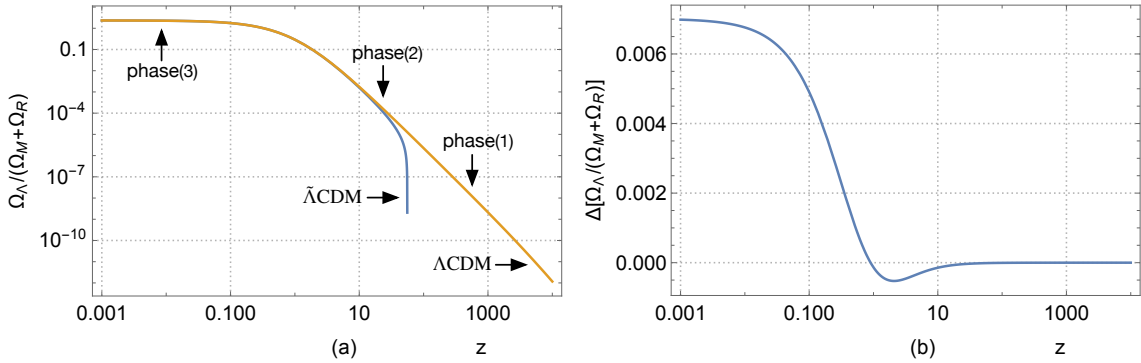


**Figure 4.** We present in left the ratio  $\rho_\Lambda/(\rho_R+\rho_M)$  (4.1) of dark energy and matter-radiation densities and in right its quantitative differences between  $\tilde{\Lambda}$ CDM and  $\Lambda$ CDM models. In phase (1), the  $\tilde{\Lambda}$ CDM ratio is about zero. The dark energy density  $\rho_\Lambda \ll \rho_{R,M}$  remains nearly zero because its interaction with matter and radiation is tiny  $\Gamma_M/H \ll 1$ . In phase (2), the  $\tilde{\Lambda}$ CDM ratio rapidly increases at  $z \sim 10$  when  $\Omega_M$  approaches to its maximum. The dark energy density closely follows up the matter and radiation densities because the interaction rate  $\Gamma_M/H$  increases. Namely, the dark energy density runs into the “tracker solution” named in the quintessence model. In phase (3), the  $\tilde{\Lambda}$ CDM ratio is only sensitive to its phase (2) behaviour and insensitive to phase (1). While the  $\Lambda$ CDM ratio depends on its behaviour in phase (1) up to the reheating end. It explains how  $\tilde{\Lambda}$ CDM evades the cosmological coincidence problem of fine-tuning the initial  $\rho_\Lambda$  value at the reheating end. Although  $\tilde{\Lambda}$ CDM and  $\Lambda$ CDM ratios approach together, they can be quantitatively different, as shown in the right figure, Figs. 2 and 3. Note that we cannot make plots in the region of small numbers due to the limit of the numerical approach.

- (iii) Figure 2 (c) shows  $\Omega_\Lambda$  evolution for  $\tilde{\Lambda}$ CDM and  $\Lambda$ CDM. The crucial difference in  $\Omega_\Lambda$  appears for  $z > 10$ . Due to the nature of constant dark energy density, the  $\Lambda$ CDM  $\Omega_\Lambda = \Lambda/(3H^2)$  dependence continues to high redshifts  $z \rightarrow z_R \gg 1$  and  $H_{RH} \gg H_0$ . Therefore, it leads the problem of fine-tuning  $\Lambda$  value for achieving  $\Omega_\Lambda^0 = \Lambda/(3H_0^2) \sim \mathcal{O}(1)$  from  $\Omega_\Lambda = \Lambda/(3H_{RH}^2) \ll \mathcal{O}(1)$ . However, this is not the case for the  $\tilde{\Lambda}$ CDM  $\Omega_\Lambda = \tilde{\Lambda}(z)/(3H^2)$ , which evolves through phases (1), (2) and (3). The present value  $\Omega_\Lambda^0$  mainly depends on variation  $\Omega_\Lambda(z)$  around small redshift  $z \sim 5$  of the phase (2). It is no longer sensitive to fine-tuning value and variation  $\Omega_\Lambda(z)$  at very large redshifts  $z \gg 1$  in phase (1), where  $\rho_\Lambda(z)$  follows up  $\rho_{R,M}(z)$  by weak interaction rate  $\Gamma_M/H \ll 1$  (3.10) and small exchange  $\delta Q \lesssim 0$  (3.11). Therefore,  $\tilde{\Lambda}$ CDM evades the  $\Lambda$ CDM fine-tuning problem of cosmological coincidence. We further show in Fig. 4 three phases (1), (2), and (3) by plotting the dark energy and matter ratio (4.1) as a function of the redshift  $z$ , respectively, for  $\tilde{\Lambda}$ CDM and  $\Lambda$ CDM models.

These discussions show that (i) apart from solving the cosmic coincidence problem, the  $\tilde{\Lambda}$ CDM’s quantities slightly deviate from the  $\Lambda$ CDM counterparts for  $z < 10^3$ ; (ii) the  $\tilde{\Lambda}$ CDM represents a one-parameter  $\tilde{m}/H_0$  extension to the  $\Lambda$ CDM model.

## 5.2 Distinct from other dark-energy interacting models

We have to point out that dynamical equation (3.7-3.9) and  $\delta Q$  (3.11) differ from general modelling dark energy and matter interactions based on total mass-energy conservation and introducing the dark and matter energy's exchange  $\delta Q_{\text{int}} \propto H\rho$ , where  $\rho$  relates to energy density, see review [12, 14]. In comparison, we find the crucial differences between the  $\tilde{\Lambda}$ CDM and interacting dark energy model:

- (i) the  $\tilde{\Lambda}$ CDM interacting term  $\delta Q$  (3.11) changes its sign depending on the dark energy converting to matter or inverse process, while the dark energy interacting model  $\delta Q_{\text{int}} \propto H\rho$  does not change the sign in evolution;
- (ii) the  $\tilde{\Lambda}$ CDM interacting rate (3.10) non-linearly relates to  $1/H$ , see Figs. 1 (f), (h), and (j) in different phases, while dark energy interacting models'  $\delta Q_{\text{int}} \propto H$  proportionally.

The difference (ii) shows that in the  $\tilde{\Lambda}$ CDM scenario, the dark energy and matter interacting rate is small in the early time of large redshift and becomes large in small redshift for the later time. As shown in Secs. 4.1 and 4.2, it is an important feature for evading the fine-tuning problem of cosmological coincidence.

## 5.3 Comparison with quintessence tracker solutions

The comparisons between the  $\tilde{\Lambda}$ CDM “following-up” solution and quintessence “tracker” solution [2] are as follows. Since dark energy density follows below radiation and matter energy densities for most of the history of the universe, both solutions are insensitive to initial conditions (values) at high redshifts and converge to the standard cosmology at low redshifts. The tracker solution differs from the self-adjusting attractor solution approaching a fixed point of autonomous differential equations of dynamical system [2]. Also, the  $\tilde{\Lambda}$ CDM solution is not an attractor solution of dynamical equations (3.7-3.9).

On the contrary to the  $\tilde{\Lambda}$ CDM scenario, there is no particle production for matter or radiation in the quintessence of cosmological scalar field  $\phi$ , which represents the dark energy component. The decrease in the scalar field  $\phi$  potential energy, rolling down the potential  $V(\phi)$ , is converted to its kinetic energy. The tracker solution is a peculiar rolling-down solution, which maintains condition  $V''(\phi) \propto H^2$  in the background density of matter and radiation. The ratio  $\rho_\phi/(\rho_R + \rho_M)$  changes steadily. How and where the scalar field  $\phi$  runs into the tracker solution depends on the potential  $V(\phi)$  and parameters. It differs from the  $\tilde{\Lambda}$ CDM scenario based on the nontrivial redshift dependent interaction (3.7-3.9) between dark energy and background energy of radiation/matter in phases (1), (2) and (3), as indicated in Figs. 1 and 4.

## 5.4 Approximated $\tilde{\Lambda}$ CDM solution for phenomenological studies

Our results base on numerical solutions to  $\tilde{\Lambda}$ CDM differential equations (3.6-3.9). Therefore, it is not convenient in practice for quantitatively comparing the  $\tilde{\Lambda}$ CDM numerical solutions with observation data. We look for approximate analytical solutions.

In redshifts  $z < 10^3$ , the interacting rate  $\Gamma_M/H$  and energy exchange  $\delta Q$  are small see Figs. 1 (h) and (j). We approximate the  $\tilde{\Lambda}$ CDM quantities as scaling factors  $(1+z)^\delta$  corrected  $\Lambda$ CDM counterparts<sup>6</sup>. The scaling indexes  $|\delta| \ll 1$ , because the  $\tilde{\Lambda}$ CDM approaches  $\Lambda$ CDM, as shown in Fig. 2. Therefore, we approximately decouple Eqs. (3.1-3.3) into

$$\dot{\rho}_\Lambda + 0H\rho_\Lambda \approx +\delta_\Lambda H\rho_\Lambda, \quad (5.4)$$

$$\dot{\rho}_M + 3H\rho_M \approx -\delta_R^G H\rho_M, \quad (5.5)$$

$$\dot{\rho}_R + 4H\rho_R \approx -\delta_M^G H\rho_R. \quad (5.6)$$

Three new dimensionless parameters  $\delta_R^G$ ,  $\delta_M^G$  and  $\delta_\Lambda$  are proportional to  $\chi\bar{m}/H_0$ , and much smaller than the unity. Equations (5.4-5.6) yield the effectively corrected densities

$$\rho_R \approx \rho_R^0(1+z)^{4-\delta_G^R}, \quad \rho_M \approx \rho_M^0(1+z)^{3-\delta_G^M}, \quad \rho_\Lambda \approx \rho_\Lambda^0(1+z)^{\delta_\Lambda}, \quad (5.7)$$

and the Hubble function

$$E^2(z) = \Omega_R^0(1+z)^{4-\delta_G^R} + \Omega_M^0(1+z)^{3-\delta_G^M} + \Omega_\Lambda^0(1+z)^{\delta_\Lambda}. \quad (5.8)$$

The equation (2.5) or (2.1,2.2) gives the constraint of parameters  $\delta_R^G$ ,  $\delta_M^G$  and  $\delta_\Lambda$ ,

$$\delta_\Lambda \approx (\Omega_M^0\delta_G^M + \Omega_R^0\delta_G^R)/\Omega_\Lambda^0, \quad (5.9)$$

and two parameters are independent. In the view of Eqs. (5.7), we find the equations of states effectively modify:  $\omega_R^{\text{eff}} \approx (1/3)(1-\delta_G^R)$ ,  $\omega_M^{\text{eff}} \approx -(1/3)\delta_G^M$  and  $\omega_\Lambda^{\text{eff}} \approx -1+(1/3)\delta_\Lambda$ , see also Ref. [37]. Equations (5.7,5.8,5.9) are  $\tilde{\Lambda}$ CDM approximate solutions, which facilitate data analysis for comparing  $\tilde{\Lambda}$ CDM with observational data.

References [38, 39] presents detailed numerical studies and data analysis based on the approximated  $\tilde{\Lambda}$ CDM solutions (5.7,5.8,5.9) and numerous data sets of observations. It shows that both  $\Lambda$ CDM  $H_0$  and  $S_8$  tensions reduces to  $2\sigma$  level with constraint parameters  $\delta_G^R \approx -1.5 \times 10^{-2}$ ,  $\delta_G^M \approx -5.0 \times 10^{-4}$  and  $\delta_\Lambda \approx -2.0 \times 10^{-4}$ . The negative parameter values support the scenario of energy conversion from radiation and matter to dark energy, as discussed in the previous section. The negative  $\delta_\Lambda \lesssim 0$  implies that due to interactions, dark energy slightly behaves as if it was a phantom energy  $\omega_\Lambda^{\text{eff}} \approx -1+(1/3)\delta_\Lambda \lesssim -1$ . It differs from the situation in inflation and reheating when dark energy converts to matter and radiation energies [22] see Fig. 5, dark energy behaves as if it was a quintessence energy  $\omega_\Lambda^{\text{eff}} > -1$ .

## 6 Discussions on Einstein cosmological $\Lambda$ term

We end this article by recalling how  $\tilde{\Lambda}$ CDM inflation and reheating processes arrive at the condition  $\rho_R \gg \rho_M \gg \rho_\Lambda$  (4.3) at the reheating end. We have studied this issue in

<sup>6</sup>In Ref. [25], we expected these dynamics and approximately derive analytical solutions (5.7,5.8) in the spirit of asymptotic safety of gravitational theories [36]. The view of scaling-law  $(1+z)^\delta$  corrections agrees to the small parameter  $\chi\bar{m}/H_0$  in the dark energy and matter interacting rate (3.10).

Refs. [21, 22]. Massive pairs' production slows down inflation driven by dark energy, and their decay to relativistic particles leads to the condition (4.3).

In addition, we present some speculations on the gravitational (geometric) and dynamical natures of the cosmological  $\tilde{\Lambda}$  term and dark-energy density  $\rho_\Lambda = \tilde{\Lambda}/(8\pi G)$  of the Einstein theory. Then, we discuss the dynamical solution to the cosmic fine-tuning problem.

## 6.1 Geometric nature of $\tilde{\Lambda}$ dark energy as gravitational ground state

The  $\tilde{\Lambda}$  term possibly represents [25, 40–44] the non-trivial ground state (Wheeler spacetime foam [45, 46]) of the spacetime. The perturbative quantum gravitational field fluctuates upon such a ground state, and the classical gravitational field varies in such a ground state. They are effectively described by the gravitation coupling  $G$ , the  $\tilde{\Lambda}$ , and the Ricci scalar  $R$  terms in Einstein's theory. Such a ground state is probably a coherent state of the long-ranged holonomy field (see Eq. (133) of Ref. [42]). It is a condensate state due to violent quantum gravity at the Planck scale. The spacetime foam structure of such a ground state is most intriguing. It could be an interacting gas of gravitational instantons (wormholes), whose effective equation of state behaves as  $p_\Lambda = -\rho_\Lambda$ , see Sec. X of Ref. [47]. We are proceeding with further studies on these aspects.

The  $\tilde{\Lambda}$  ( $\xi \sim 1/\tilde{\Lambda}^{1/2}$ ) is the characteristic scale (correlation length) of such non-trivial geometric ground state [25, 44]. It represents the intrinsic scale for effective gravitational field theories realized in the scaling domains of fixed points of effective gravitational coupling  $g \sim GM_{\text{pl}}^2$  to matter and radiation. The  $\tilde{\Lambda}$  and  $g$  varying from one fixed point to another render its dynamic nature. It is nontrivial to demonstrate these dynamical features. However, as analogies, we mention fundamental field theories of interactions (i) the electroweak scale  $v \sim 10^2 \text{ GeV}$  for electroweak field theory realized in the scaling domain of infrared (IR) fixed point; (ii) the scale  $\Lambda_{\text{QCD}} \sim 10^2 \text{ MeV}$  for perturbative QCD field theory realized in the scaling domain of ultraviolet (UV) fixed point; (iii) the low-energy hadron scale for non-perturbative QCD field theory realized in the scaling domain of IR fixed point.

## 6.2 Asymptotically safe Einstein theory for early and present Universe

On the one hand, in early Universe of  $\tilde{\Lambda}$  dark energy dominated inflation,  $H^2 \sim (8\pi G/3)\rho_\Lambda$  and  $\rho_\Lambda = \tilde{\Lambda}/(8\pi G)$  asymptotically give  $\xi \sim 1/\tilde{\Lambda}^{1/2} \sim H^{-1}$ . Namely, the correlation length  $\xi$  is the size of the horizon. The  $\tilde{\Lambda}^{1/2}$  slowly varies from the inflation scale  $H^*$  to the scale  $H_{\text{end}} \approx (0.42, 0.35)H_*$  at inflation end  $a_{\text{end}}$ . The  $H_* \sim 10^{-6}M_{\text{pl}}$  is obtained from the CMB data, see Eqs. (6.5) and (6.10) of Ref. [21]. The inflation scale  $H_*$  is much smaller than the Planck scale. How quantum gravitation field theory with the intrinsic scale  $\tilde{\Lambda}^{1/2} \sim M_{\text{pl}}$  runs to the effective Einstein theory at the scale  $\tilde{\Lambda}^{1/2} \sim H_* \ll M_{\text{pl}}$ . How does the quantum gravity ground state evolve to the  $\tilde{\Lambda}$  ground state of effective Einstein theory? One could study it in the context of the asymptotically safe and effective theories of gravitation [36] and the scaling domain of a UV unstable fixed point [25].

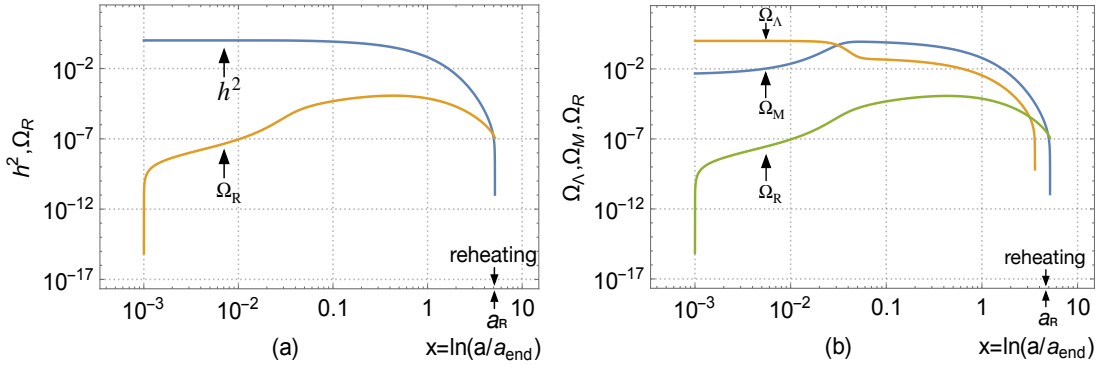


**Figure 5.** We reproduce the  $\tilde{\Lambda}$ CDM results of the Hubble function  $h^2 = H^2/H_{\text{end}}^2$  (left),  $\Omega_M$ ,  $\Omega_R$  and  $\Omega_\Lambda$  (right) in reheating, see Figure 6 (a) and (b) in Ref. [22]. They are in the unit of  $\rho_c^{\text{end}} = 3m_{\text{pl}}^2 H_{\text{end}}^2$  and the Hubble scale  $H_{\text{end}} \approx (0.42, 0.35)H_*$  at inflation end  $a_{\text{end}}$ , see Eq. (6.10) of Ref. [21]. The parameters  $\hat{m}/m_{\text{pl}} \approx 27.7$  and  $\chi \approx 1.85 \times 10^{-3}$ . It shows that in a few numbers  $x = \ln(a/a_{\text{end}})$ , dark energy  $\Omega_\Lambda$  decreases from one to zero because of rapidly converting to matter and radiation. Matter  $\Omega_M$  increases and dominates over  $\Omega_\Lambda$ . Then  $\Omega_M$  decreases because of decaying to radiation  $\Omega_R$ . As a result,  $\Omega_R$  increases and becomes dominant. At the reheating end  $(a_R/a_0) = (1 + z_R)^{-1}$ , the radiation abundance is about one, and the dark energy and matter abundances are about zero.

On the other hand, in the recent Universe of  $\tilde{\Lambda}$  dark energy dominated acceleration,  $H_0^2 \sim (8\pi G/3)\rho_\Lambda^0$  asymptotically gives the scale  $\xi \sim 1/\tilde{\Lambda}^{1/2} \sim H_0^{-1}$  and density  $\rho_\Lambda^0 \approx H_0^2/(8\pi G)$  [48]. Based on the same spirit of asymptotic safety of effective gravitational theories [36], we study its realization in the scaling domain of a UV stable fixed point, where is the effective Einstein theory of relevant operators  $R/G$  and  $\tilde{\Lambda}/G$ , and gravitational coupling  $G$  and cosmological  $\tilde{\Lambda}$  approach their values today [25, 44]. However, due to the dark energy, radiation and matter interactions, as well as pair production of massive particles and antiparticles on the horizon, it is nontrivial to find the scaling laws for operators  $R/G$  and  $\tilde{\Lambda}/G$  by using the asymptotic safety principle. The questions are how the  $\tilde{\Lambda}$  dark energy varies from the inflation scale  $H_*$  to the recent Hubble scale  $H_0 \ll H_*$ . How the dark energy density changes from  $\rho_\Lambda^* \approx H_*^2/(8\pi G)$  to  $\rho_\Lambda^0 \ll \rho_\Lambda^*$  in many orders of magnitudes. We use the  $\tilde{\Lambda}$ CDM solutions in inflation, reheating and standard cosmology to explain the possible solution to such cosmic fine-tuning problem.

### 6.3 Dynamical nature of $\tilde{\Lambda}$ dark energy solving fine-tuning problem

After the inflation ends, the Universe undergoes reheating. Based on dynamical equations (3.6-3.9), we show [22] that due to strong coupling ( $\Gamma_M/H \gg 1$ ) between  $\tilde{\Lambda}$  dark energy and matter energy densities, dark energy rapidly converts into massive matter, and the latter decays to radiation energy. As a result, dark energy density decreases from  $\rho_\Lambda^{\text{end}} \approx 3m_{\text{pl}}^2 H_{\text{end}}^2$  to  $\rho_\Lambda^R \approx 0$ , where  $\rho_{\Lambda, M, R}^R$  stand for the dark energy, matter and radiation densities at the reheating end  $a_R/a_0 = (1 + z_R)^{-1}$ . We illustrate in Fig. 5 the dynamical reheating process from the inflation end  $\rho_\Lambda^{\text{end}} \gg \rho_M^{\text{end}} \gg \rho_R^{\text{end}} \approx 0$  to

the reheating end  $\rho_R^R \gg \rho_M^R \gg \rho_\Lambda^R \approx 0$ . The radiation energy density  $\rho_R^R$  becomes dominant, initiating the standard cosmology. There is no fine-tuning in this process.

Then how the standard cosmology dynamically evolves to the coincidence  $\rho_\Lambda^0 \sim \rho_M^0 \gg \rho_R^0 \approx 0$  in the recent epoch. It is the issue addressed in this article. The initial values of the scale factor  $a_R$ , Hubble constant  $H_{\text{RH}}$  and energy densities  $\rho_{R,M,\Lambda}^R$  cannot be completely determined. Therefore, we cannot uniquely solve ordinary differential equations (3.6-3.9) from the reheating end  $z_R$  to the present epoch  $z = 0$ . However, we use the present values (3.12) to uniquely solve ordinary differential equations (3.6-3.9) from today  $z = 0$  back to the reheating end  $z_R \gg 0$ . As shown in Fig. 1 (b) and Fig. 2 (c), the dynamical solutions asymptotically approach the same initial conditions  $\rho_R^R \gg \rho_M^R \gg \rho_\Lambda^R \approx 0$  for  $z \rightarrow z_R \gg 1$  without any fine-tuning.

Such qualitative matching implies a consistent dynamical solution for the cosmic fine-tuning problem in the following way. Converting to matter and radiation  $\delta Q \gg 1$  (3.11), the dark energy density decreases from the inflation scale  $\rho_\Lambda^* \approx 3m_{\text{pl}}^2 H_*^2$  to inflation end  $\rho_\Lambda^{\text{end}} \approx 3m_{\text{pl}}^2 H_{\text{end}}^2$ , then to reheating end  $\rho_\Lambda^R \approx 0$ . Since the standard cosmology starts, converted from matter and radiation  $\delta Q \lesssim 0$  (3.11), the dark energy density increases from the reheating end value  $\rho_\Lambda^R \approx 0$  to the present value  $\rho_\Lambda^0 \approx H_0^2/(8\pi G)$  [48]. Such a dynamical evolution is free from fine-tuning. It can be the solution to the cosmic coincidence problem. The basic reasons are that in evolution dark energy and matter conversion  $\delta Q$  (3.11) changes sign and is proportional to the interacting rate  $\Gamma_M/H \propto \chi m\epsilon/H$  and  $m > H$ .

Nonetheless, we have not yet found the complete and quantitative solution to the cosmic fine-tuning problem since we separately adopt the effective values of mass parameter  $m_*/H_*$  for inflation,  $\hat{m}/H_{\text{end}}$  for reheating and  $\bar{m}/H_0$  for standard cosmology. The mass parameter  $m$  is proportional to the mass  $M$  and number  $\mathcal{N}_{\text{pair}}$  of massive particle and antiparticle pairs in the holographic massive plasma state. Therefore, its value should depend on the horizon  $H$ , i.e.,  $m = m(H)$ . Its time-varying should be slower than the  $H$  so that the dark energy and matter interacting rate  $\Gamma_M/H \propto m(H)/H \propto m_{\text{eff}}/H$  decreases (increases) as  $H$  increases (decreases). We have not been able to determine  $m(H)$  in theory. Instead, we define its effective values  $m_{\text{eff}}$  of each epoch, for instance,  $m_{\text{eff}}^R$  for radiation domination and  $m_{\text{eff}}^M$  for matter domination, whose values should be fixed by observations. To understand these fundamental natures of the Einstein cosmological  $\Lambda$  term in cosmology, further observations of the cosmos are necessary [49, 50].

## 7 Appendix: quantum pair oscillation details

We add this appendix for readers' convenience to gain a preliminary picture of massive pair productions and oscillations without going into details of Ref. [21, 22]. We show the massive particle production and oscillation coupling with the Hubble function fast component  $H_{\text{fast}}$ . For a given  $H$  and  $h^{\text{fast}} = H_{\text{fast}}/H$ , we express in unit of the critical density  $\rho_{\text{crit}} = 3m_{\text{pl}}^2 H^2$  the dimensionless quantum pressure  $\mathcal{P}_M^{\text{fast}}$  and density  $\varrho_M^{\text{fast}}$ . In dimensionless microscopic time  $t$  in the unit of  $M^{-1}$ , we plot the Bogoliubov coefficient  $|\beta|^2$ , the quantum pair density  $\varrho_M^{\text{fast}}$  and pressure  $\mathcal{P}_M^{\text{fast}}$ , as well as the fast components

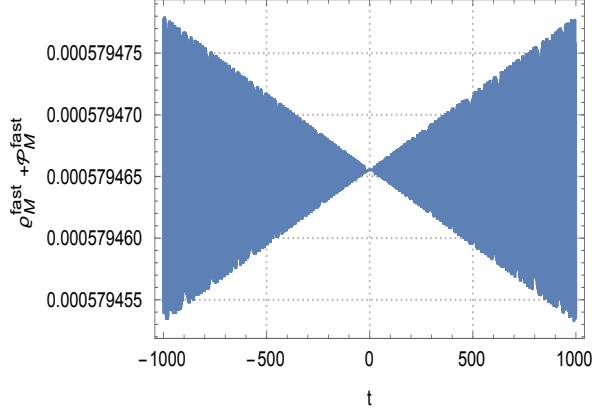


**Figure 6.** We show the quantum pair density and pressure oscillations in microscopic time  $t$  in the unit of  $M^{-1}$ , using  $H/M \approx 10^{-3}$ ,  $M \simeq 10^{-10}m_{\text{pl}}$ ,  $\mathcal{N}_{\text{pair}} \simeq 2 \times 10^{22}$  and  $\delta = 1$ . It shows that a large number of massive pairs creates significant oscillating quantum pressure  $\mathcal{P}_M^{\text{fast}}$  and  $\varrho_M^{\text{fast}}$  in the unit of  $\rho_{\text{crit}} = 3m_{\text{pl}}^2 H^2$ . In this coherent state,  $\mathcal{P}_M^{\text{fast}}$  and  $\varrho_M^{\text{fast}}$  oscillation frequency is about  $M$ . Their oscillating amplitudes  $\delta\varrho_M^{\text{fast}}/\varrho_M^{\text{fast}}$  and  $\delta\mathcal{P}_M^{\text{fast}}/\mathcal{P}_M^{\text{fast}}$  are about  $\mathcal{O}(10^{-3})$ . For a long time, the coherent oscillations approach stable configurations in time. Note that the pair number  $\mathcal{N}_{\text{pair}}$ , mass scales  $M$  and  $H$  values differ from those used for inflation see Fig. 1 in Ref. [21] and reheating see Fig. 1 in Ref. [22].

of the Hubble function  $h_{\text{fast}}$ , and cosmological term  $\varrho_{\Lambda}^{\text{fast}}$ . The details and notations are given in Secs. 2-3 of Ref. [22].

In Figs. 1, 3 and 4 of Ref. [21], we show the features of dynamical oscillation in pre-inflation and inflation epochs for the mass parameter  $m_* \approx 3.1m_{\text{pl}}$ . In Figs. 1 and 11 of Ref. [22], we show the features of dynamical oscillation reheating epoch for the parameter  $\hat{m} \approx 20m_{\text{pl}}$ . While for the standard cosmology after reheating, both the Hubble scale  $H$  and pair mass  $M$  are very much smaller than the Planck mass, i.e.,  $H \ll M \ll m_{\text{pl}}$  and pair number  $\mathcal{N}_{\text{pair}} \gg 1$ . Therefore, we present these plots for the selected values  $H/M$  and  $\mathcal{N}_{\text{pair}}$ , which differ from those in inflation and reheating. It also gives an insight into the mass parameter  $m$  variation from one epoch to another.

## References

- [1] S. Weinberg, *The cosmological constant problem*, *Rev. Mod. Phys.* **61** (1989) 1.
- [2] I. Zlatev, L.-M. Wang and P. J. Steinhardt, *Quintessence, cosmic coincidence, and the cosmological constant*, *Phys. Rev. Lett.* **82** (1999) 896 [[astro-ph/9807002](#)].
- [3] G. Huey and B. D. Wandelt, *Interacting quintessence. the coincidence problem and cosmic acceleration*, *Phys. Rev. D* **74** (2006) 023519 [[astro-ph/0407196](#)].
- [4] H. E. S. Velten, R. F. vom Marttens and W. Zimdahl, *Aspects of the cosmological “coincidence problem”*, *Eur. Phys. J. C* **74** (2014) 3160 [[1410.2509](#)].

- [5] R. R. Caldwell, R. Dave and P. J. Steinhardt, *Cosmological imprint of an energy component with general equation of state*, *Phys. Rev. Lett.* **80** (1998) 1582 [[astro-ph/9708069](#)].
- [6] P. J. Steinhardt, *Quintessential ideas*, *Phys. Scripta T* **117** (2005) 34.
- [7] L. Amendola, *Coupled quintessence*, *Phys. Rev. D* **62** (2000) 043511 [[astro-ph/9908023](#)].
- [8] L. Amendola and S. Tsujikawa, *Dark Energy: Theory and Observations*. Cambridge University Press, 1, 2015.
- [9] C. G. Boehmer, G. Caldera-Cabral, R. Lazkoz and R. Maartens, *Dynamics of dark energy with a coupling to dark matter*, *Phys. Rev. D* **78** (2008) 023505 [[0801.1565](#)].
- [10] J. Valiviita, E. Majerotto and R. Maartens, *Instability in interacting dark energy and dark matter fluids*, *JCAP* **07** (2008) 020 [[0804.0232](#)].
- [11] S. del Campo, R. Herrera and D. Pavon, *Interacting models may be key to solve the cosmic coincidence problem*, *JCAP* **01** (2009) 020 [[0812.2210](#)].
- [12] B. Wang, E. Abdalla, F. Atrio-Barandela and D. Pavon, *Dark matter and dark energy interactions: Theoretical challenges, cosmological implications and observational signatures*, *Rept. Prog. Phys.* **79** (2016) 096901 [[1603.08299](#)].
- [13] Y. L. Bolotin, A. Kostenko, O. A. Lemets and D. A. Yerokhin, *Cosmological evolution with interaction between dark energy and dark matter*, *Int. J. Mod. Phys. D* **24** (2014) 1530007 [[1310.0085](#)].
- [14] E. Di Valentino, A. Melchiorri, O. Mena and S. Vagnozzi, *Interacting dark energy in the early 2020s: A promising solution to the  $H_0$  and cosmic shear tensions*, *Phys. Dark Univ.* **30** (2020) 100666 [[1908.04281](#)].
- [15] E. Di Valentino, A. Melchiorri, O. Mena and S. Vagnozzi, *Nonminimal dark sector physics and cosmological tensions*, *Phys. Rev. D* **101** (2020) 063502 [[1910.09853](#)].
- [16] S. Pan, J. de Haro, W. Yang and J. Amorós, *Understanding the phenomenology of interacting dark energy scenarios and their theoretical bounds*, *Phys. Rev. D* **101** (2020) 123506 [[2001.09885](#)].
- [17] S. Pan, G. S. Sharov and W. Yang, *Field theoretic interpretations of interacting dark energy scenarios and recent observations*, *Phys. Rev. D* **101** (2020) 103533 [[2001.03120](#)].
- [18] M. Lucca and D. C. Hooper, *Shedding light on dark matter-dark energy interactions*, *Phys. Rev. D* **102** (2020) 123502 [[2002.06127](#)].
- [19] M. Lucca, *Dark energy–dark matter interactions as a solution to the  $S_8$  tension*, *Phys. Dark Univ.* **34** (2021) 100899 [[2105.09249](#)].



- [20] N. Dalal, K. Abazajian, E. E. Jenkins and A. V. Manohar, *Testing the cosmic coincidence problem and the nature of dark energy*, *Phys. Rev. Lett.* **87** (2001) 141302 [[astro-ph/0105317](#)].
- [21] S.-S. Xue, *Massive particle pair production and oscillation in Friedman universe: its effect on inflation*, *Eur. Phys. J. C* **83** (2023) 36 [[2112.09661](#)].
- [22] S.-S. Xue, *Massive particle pair production and oscillation in Friedman universe: reheating energy and entropy, and cold dark matter*, *Eur. Phys. J. C* **83** (2023) 355 [[2006.15622](#)].
- [23] V. Salvatelli, N. Said, M. Bruni, A. Melchiorri and D. Wands, *Indications of a late-time interaction in the dark sector*, *Phys. Rev. Lett.* **113** (2014) 181301 [[1406.7297](#)].
- [24] S. Gariazzo, E. Di Valentino, O. Mena and R. C. Nunes, *Late-time interacting cosmologies and the Hubble constant tension*, *Phys. Rev. D* **106** (2022) 023530 [[2111.03152](#)].
- [25] S.-S. Xue, *How universe evolves with cosmological and gravitational constants*, *Nucl. Phys. B* **897** (2015) 326 [[1410.6152](#)].
- [26] L. Parker and S. A. Fulling, *Quantized matter fields and the avoidance of singularities in general relativity*, *Phys. Rev. D* **7** (1973) 2357.
- [27] A. A. Starobinsky, *Nonsingular model of the universe with the quantum-gravitational de sitter stage and its observational consequences*, *Proc. of the Second Seminar "Quantum Theory of Gravity"*, Moscow, October 1981, INR Press, Moscow (1982) 58.
- [28] L. H. Ford, *Gravitational particle creation and inflation*, *Phys. Rev. D* **35** (1987) 2955.
- [29] D. J. H. Chung, P. Crotty, E. W. Kolb and A. Riotto, *On the gravitational production of superheavy dark matter*, *Phys. Rev. D* **64** (2001) 043503 [[hep-ph/0104100](#)].
- [30] D. J. H. Chung, E. W. Kolb and A. J. Long, *Gravitational production of super-Hubble-mass particles: an analytic approach*, *JHEP* **01** (2019) 189 [[1812.00211](#)].
- [31] Q. Wang and W. G. Unruh, *Vacuum fluctuation, microcyclic universes, and the cosmological constant problem*, *Phys. Rev. D* **102** (2020) 023537 [[1904.08599](#)].
- [32] Q. Wang, *Reformulation of the cosmological constant problem*, *Phys. Rev. Lett.* **125** (2020) 051301 [[1904.09566](#)].
- [33] S.-S. Xue, *Cosmological  $\Lambda$  driven inflation and produced massive particles*, [1910.03938](#).
- [34] S.-S. Xue, *Cosmological constant, matter, cosmic inflation and coincidence*, *Mod. Phys. Lett. A* **35** (2020) 2050123 [[2004.10859](#)].
- [35] J. Mielczarek, *Reheating temperature from the CMB*, *Phys. Rev. D* **83** (2011) 023502 [[1009.2359](#)].

- [36] S. Weinberg, *Asymptotically safe inflation*, *Phys. Rev. D* **81** (2010) 083535 [[0911.3165](#)].
- [37] D. Bégué, C. Stahl and S.-S. Xue, *A model of interacting dark fluids tested with supernovae and baryon acoustic oscillations data*, *Nucl. Phys. B* **940** (2019) 312 [[1702.03185](#)].
- [38] L.-Y. Gao, Z.-W. Zhao, S.-S. Xue and X. Zhang, *Relieving the  $H_0$  tension with a new interacting dark energy model*, *JCAP* **07** (2021) 005 [[2101.10714](#)].
- [39] L.-Y. Gao, S.-S. Xue and X. Zhang, *Dark energy and matter interacting scenario can relieve  $H_0$  and  $S_8$  tensions*, *Chinese Physics C* **Vol. 48, No. 6** (2024) 051001 [[2212.13146](#)].
- [40] S. R. Coleman, *Why there is nothing rather than something: A theory of the cosmological constant*, *Nucl. Phys. B* **310** (1988) 643.
- [41] A. O. Barvinsky, *Why there is something rather than nothing (out of everything)?*, *Phys. Rev. Lett.* **99** (2007) 071301 [[0704.0083](#)].
- [42] S.-S. Xue, *Detailed discussions and calculations of quantum Regge calculus of Einstein-Cartan theory*, *Phys. Rev. D* **82** (2010) 064039 [[0912.2435](#)].
- [43] S.-S. Xue, *Quantum Regge calculus of Einstein-Cartan theory*, *Phys. Lett. B* **682** (2009) 300 [[0902.3407](#)].
- [44] S.-S. Xue, *The phase and critical point of quantum Einstein-Cartan gravity*, *Phys. Lett. B* **711** (2012) 404 [[1112.1323](#)].
- [45] C. W. Misner, K. S. Thorne and J. A. Wheeler, *Gravitation*. W. H. Freeman, San Francisco, 1973.
- [46] S. Carlip, *Spacetime foam: a review*, [2209.14282](#).
- [47] S.-S. Xue, *Gravitational instanton and cosmological term*, *Int. J. Mod. Phys. A* **24** (2009) 3865 [[hep-th/0608220](#)].
- [48] V. G. Gurzadyan and S.-S. Xue, *On the estimation of the current value of the cosmological constant*, *Mod. Phys. Lett. A* **18** (2003) 561 [[astro-ph/0105245](#)].
- [49] EUCLID THEORY WORKING GROUP collaboration, *Cosmology and fundamental physics with the Euclid satellite*, *Living Rev. Rel.* **16** (2013) 6 [[1206.1225](#)].
- [50] L. Amendola et al., *Cosmology and fundamental physics with the Euclid satellite*, *Living Rev. Rel.* **21** (2018) 2 [[1606.00180](#)].

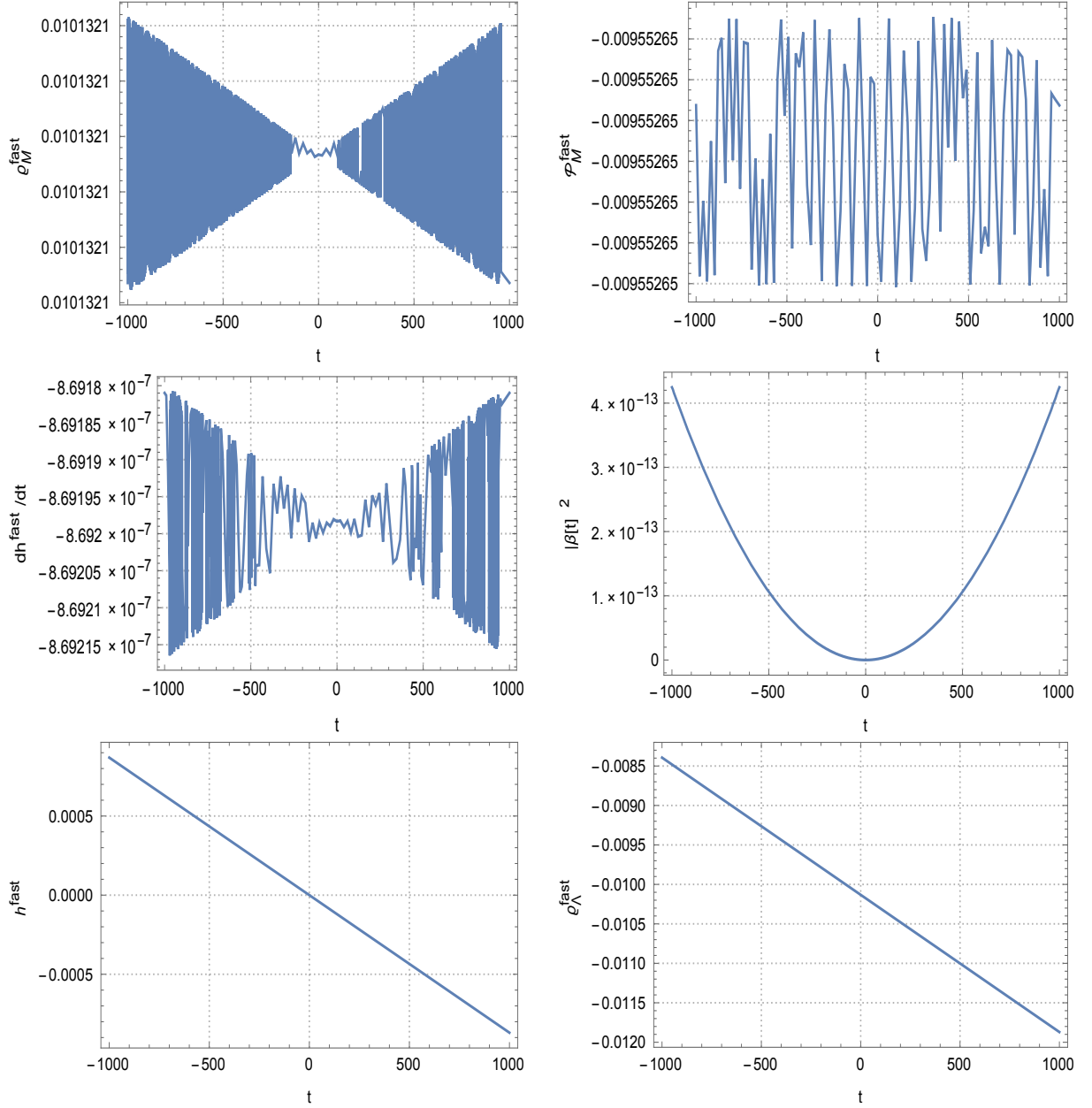


**Figure 7.** Corresponding to Fig. 6, we show the details of quantum pair oscillation in microscopic time  $t$  in the unit of  $M^{-1}$ . The oscillatory  $|\beta(t)|^2$ ,  $h_{\text{fast}} = H_{\text{fast}}/H$  and  $\varrho_\Lambda^{\text{fast}}$  structures are too small to see. The parameters' values are the same as those in Fig. 6. The non-smooth curve  $|\beta(t)|^2$  shows its oscillating behaviour. The  $h_{\text{fast}}$  and  $\varrho_\Lambda^{\text{fast}}$  oscillatory structures are too small to see due to the precision limit for numerical calculations with the parameters' values used. However, one can infer their oscillating behaviours by the oscillating  $dh^{\text{fast}}/dt$ . We suggest readers see Fig. 4 of Ref. [21] for pre-inflation and inflation, where the corresponding solutions for other parameters' values and plotting scales show evident oscillatory structures.